On the Dependence of Hindcast Skill on Ocean Thermodynamics in a Coupled Ocean–Atmosphere Model

RICHARD KLEEMAN

Bureau of Meteorology Research Centre, Melbourne, Australia

(Manuscript received 17 July 1992, in final form 19 February 1993)

ABSTRACT

Three different mechanisms for the generation of ENSO SST anomalies within a simplified tropical Pacific Ocean model are examined: thermocline depth changes, Ekman-induced upwelling anomalies, and zonal advection changes. The effect of varying the relative influence of these terms on the realism of tropical Pacific coupled models is analyzed. The principal tool used to assess such realism is hindcast skill, with forced ocean and oscillatory behavior also being examined. Of the mechanisms considered, thermocline perturbations are shown to be crucially important for high coupled-model hindcast skill. Furthermore, it is concluded that the realism of the model (as measured by hindcast skill) deteriorates markedly when the influence on SST of Ekman upwelling becomes greater than a small fraction of the thermocline influence. This provides strong evidence for the hypothesis that Ekman upwelling anomalies (which are essentially a local response to wind stress anomalies) have only a small influence on the creation of real world SST anomalies. The implications of this latter point for coupled models involving ocean general circulation models is briefly discussed. It is also demonstrated that western boundary reflections provide a vital role by means of a negative feedback in ensuring realistic performance. The hindcast skill (as measured by NINO3 anomaly correlation) demonstrated by a model involving only the thermocline mechanism can be tuned to exceed that of the benchmark Cane and Zebiak model for hindcast lags up to 7 months (from 7 to 12 months the model skills are roughly equal).

1. Introduction

In the past 5 to 10 years extensive activity has taken place in the area of the modeling and theoretical analysis of tropical ocean–atmosphere coupling. Such activity is generally accepted as being crucial in the development of our capability for forecasting the large climate perturbations associated with ENSO (El Niño–Southern Oscillation).

In general the focus of modeling studies has been on demonstrating variability on interannual time scales and a wide variety of such behavior has been observed (see, e.g., Anderson and McCreary 1985; Zebiak and Cane 1987; Meehl 1990; Neelin 1990; and Philander et al. 1992). At the same time, theoretical analyses have indicated a variety of possible mechanisms for the generation of such variability (see, e.g., Philander et al. 1984; Hirst 1986; Battisti 1988; Suarez and Schopf 1988; Hirst 1990; and Neelin 1991). It remains unclear, however, how much connection model oscillations and proposed mechanisms have with the real world coupled ocean–atmosphere system. It is, of course, often argued that all mechanisms play some role in nature and no doubt there is truth in such an assertion. Nevertheless it would be useful if an indication of which processes are of *primary* importance could be obtained. It is fairly clear that in order to achieve such an object, methods for assessing the veracity of coupled models are required.

One way of tackling such a task, recently advocated by Chao and Philander (1991), is to carefully assess the spatial and temporal structure of the important variables in the coupled oscillation [for example, sea surface temperature (SST), wind, and upper-level heat content], then compare them to observations and forced model runs. Important differences are then an indication of the limitation of the coupled behavior. Another, perhaps more objective, method of assessment is that recently used by Goswami and Shukla (1991) and also Latif and Flügel (1991) in which the hindcast skill of the model is evaluated by making a statistically significant number of hindcasts. Such a method should, in principle, give quite a clear indication of how well a given coupled model is simulating the primary mechanism of coupled behavior in the real world. A third method for assessing the veracity of a coupled model is to subject the individual components to observed forcing from the other component (the ocean model with observed fluxes of momentum and some parameterization of heat flux; the atmospheric model with the observed SST) and then critically compare the resultant response in quantities im-

Corresponding author address: Dr. Richard Kleeman, Bureau of Meteorology Research Centre, G.P.O. Box 1289K, Melbourne, 3001, Australia.

portant for coupling. Such an approach has been adopted (using hindcasts) for an ocean general circulation model by Harrison et al. (1989). A comparison of modeled and observed empirical orthogonal functions (EOFs) is another method of implementing such an approach. Such a philosophy has been adopted by Latif and Villwock (1990) and Zebiak (1990) among others.

Perhaps the most successful model when judged against the above criteria is that of Zebiak and Cane (1987, referred to henceforth as ZC), which exhibits an interannual oscillation with a reasonable degree of realism; gives indications of hindcast skill (see Cane 1991; Goswami and Shukla 1991); and has reasonable forced behavior. Another model with some degree of success is the coupled tropical GCM of Philander et al. (1992), which displays interannual variability with a measure of realism. It is difficult to apply the second criterion of hindcast skill to this model because its coupled climatology (particularly equatorial zonal stress) is sufficiently different from the observed climatology that problems of incompatibility would be encountered at the initialization of hindcasts.

Given the wide diversity of coupled behavior currently observed in models (see Neelin et al. 1992), it would be of value to modelers to identify which physical processes are important for realistic performance so that improved representations of them could be implemented.

The aim of this contribution is to provide such information for ocean models. To this end, a fixed atmospheric model whose performance has had extensive testing with observed SSTs (see Kleeman 1991; Kleeman et al. 1992) is coupled to an ocean model whose thermodynamics are subjected to parametric variation. The resulting coupled and forced oceanic behavior is assessed using the three criteria mentioned above. Particular focus is placed on the varying hindcast skill, not only because of its objective measure of model performance, but also because of its practical application. In order to apply the hindcast test, long runs involving typically 100 years of integration per parameter setting are required. In order to make such a project feasible, simplifications are required in the ocean model. Such simplifications also aid in the interpretation of results.

The influence of ocean thermodynamics on coupled model behavior has received extensive attention in the literature in the past decade. Hirst (1986) demonstrated that varying the contributions of zonal advection and thermocline displacements in the SST equation resulted in the destabilization of coupled modes with quite different characteristics. Battisti and Hirst (1989) simplified the ZC model and explained its behavior in terms of a delay differential equation with the following essential character: A local instability in the eastern Pacific caused by the influence of zonal advection, Ekman upwelling, and thermocline displacements on SST is "controlled" by a negative feedback caused by the western boundary reflection of a thermocline displacement of the opposite sign. The "competition" between these two processes results in an oscillation, hence the so-called "delayed action oscillator." Neelin (1990) and (1991) analyzed an oscillation in a hybrid coupled GCM (a simple atmosphere coupled to an ocean general circulation model) and concluded that the instability driving the oscillation was in all probability due to the equal influence of Ekman upwelling and thermocline displacements on SST. In addition he demonstrated that wave reflections from boundaries were not crucial to the oscillation, implying that the coupled mode extant in his model was fundamentally different from the one seen in the ZC model.

The above considerations will guide us in the formulation of our SST parameterizations and sensitivity experiments. All three mechanisms for SST mentioned above will be included in the model to be discussed in the next section. In addition the effect of western boundary reflections will be examined together with a careful study of the influence on realism of the details of the parameterizations used. This latter study is being undertaken to provide assurance that the skill found is robust (i.e., not dependent on the details of the parameterization used).

The paper is organized so that in section 2 the uncoupled models are described and the various parameterizations of SST in the ocean model are derived and justified. Section 3 describes the variation in coupled model performance as the SST equation changes from being dominated by upwelling effects to being dominated by thermocline displacements. In section 4 a similar analysis is carried out for variation from thermocline-dominated to zonal advection–dominated thermodynamics. Section 5 examines model sensitivity to a number of factors involved in the ocean model parameterization: zonal asymmetry, western boundary reflections, nonlinearity, thermal relaxation time scale, and shallow-water wave speed. Finally section 6 contains a summary and discussion of results presented and their applicability to studies with general circulation models, along with suggestions for further work.

2. Uncoupled models and the coupling procedure

The atmospheric model used here has been described in detail in Kleeman (1991). Its performance has been subjected to extensive examination both there and also in Kleeman et al. (1992). In general, the model gives a good depiction of the zonal wind anomalies associated with ENSO. The only error of possible significance is in the far eastern Pacific where the model winds are probably somewhat overestimated (errors around 1 m s^{-1} are typical at the extreme phases of ENSO).

This anomaly model consists of a steady-state Gill (1980)-style dynamical component forced by direct thermal heating. The heating, which is assumed proportional to the SST anomaly, induces by feedback

a much larger latent heating derived from a vertically integrated steady-state moisture equation. The precipitation (and hence most of the heating) has a strong tendency to locate itself in regions where the total SST is high.

The major limitations/areas of uncertainty in the model are, apart from the far eastern Pacific winds, the absence of internal variability (particularly the 30–50-day Madden Julian oscillation) and the relative roles of latent and nonlatent heating. This latter factor is related to the degree of moisture feedback, which influences the model tendency to locate total heating in high SST regions. Observational evidence presented in Kleeman (1991) suggests that the precipitation response of the model is quite good. This in turn suggests little reason to question the current tuning.

The philosophy followed in constructing the anomaly Pacific Ocean model was to retain only those features thought essential for an equatorial oceanic depiction of ENSO. Thus, the first baroclinic mode shallow-water equations, on a beta plane and confined by a western boundary at 124°E and an eastern boundary at 80°W, were used to depict thermocline movements as well as part of the zonal currents. The long-wave approximation was applied and a weak dissipation in the form of Rayleigh friction and Newtonian "cooling" inserted. The stress anomalies forcing the equations were applied at a body force equivalent depth of 150 m. In addition only a small number of meridional modes were retained: namely, the Kelvin and first six Rossby modes. The shallow-water speed was chosen to be 2.8 m s^{-1} (except in section 5), which is close to observational estimates from the central equatorial Pacific. Mathematical details of the dynamics of the model and boundary conditions are very similar to those previously discussed in the literature (e.g., see Battisti 1988).

The SST anomaly equation was simplified by assuming a fixed meridional structure for anomalies. In particular, they are assumed to have a Gaussian shape centered on the equator with an e-folding radius of 10°. Such a simplification has previously been made by Neelin (1991) and reflects the assumption that meridional effects such as advection and the differing structure of horizontal modes are unimportant to the primary ENSO mechanism. Symbolically we write the equatorial SST equation as:

$$T'_t = TT(h') + EUT(w', \bar{w}) + AT(u'_m, \bar{u}_m, T', \bar{T}) - \epsilon T', \quad (2.1)$$

where T' is the equatorial SST anomaly; TT is the SST anomaly tendency due to thermocline anomalies h'; EUT is the tendency due to Ekman-induced equatorial upwelling anomalies w' and also depends on the mean such upwelling $\bar{w}$; AT is the tendency due to zonal advection changes and depends on the mean and anomalous mixed-layer currents $\bar{u}_m$ and u'_m together with the mean equatorial SST $\bar{T}$ and T'. Finally, a simple relaxation term $\epsilon T'$ is also included to model negative feedbacks such as heat flux changes and erasure of anomalies by entrainment of deep water (see Neelin 1990).

In a complete physical model of the equatorial Pacific the first two terms depend in a reasonably complex manner on the entrainment/detrainment processes of the upper-ocean mixed layer. Many different parameterizations for this process are available in the literature (see, e.g., Kraus 1977) and it is fair to say that a degree of uncertainty attaches both to the formulation of the physics of the mixed layer and to its embedding into a dynamical model (see Pacanowski and Philander 1981; Schopf and Cane 1982; and Oberhuber 1993 for a variety of approaches to the problem). The oceanic component of the ZC coupled model introduces four crucial simplifications to model the above physics: a constant (50 m) depth mixed layer; a constant (150 m) depth layer for the shallow-water equation currents; a linear formulation of the mixed-layer shear flow; and finally a prescribed time-invariant specification of thermocline structure. From these assumptions emerge fairly complex expressions for the terms in (2.1). It is unclear whether such complexity can be justified given the simplifications mentioned above and it is obvious that doubt remains about the relative contributions (and form) of each term. In the present work we choose the simplest formulation consistent with producing an SST pattern close to the observations. As shall become clear from the results described below, hindcast skill depends sensitively on the relative roles of the first two terms in (2.1), which in turn suggests that a focus on the correct formulation of mixed-layer processes (particularly entrainment) should be a high priority for ENSO studies.

We now discuss the details of the parameterizations of the various terms in equation (2.1). The values for the parameters introduced in what follows may be found in Table 1 while a discussion of the choices made may be found toward the end of this section.

We parameterize the influence of thermocline movements on SST in the following manner:

$$TT(h') = \Lambda(x)M(h'), \quad (2.2)$$

where we have defined

$$\Lambda(x) = \eta \quad \text{for} \quad x \geq 140.3°\text{W}$$
$$= \eta/eff \quad \text{for} \quad x \leq 176.7°\text{W} \quad (2.3)$$

TABLE 1. Parameter values for the ocean model.

Parameter	Value
ϵ	2.72×10^{-7} s^{-1}
η (maximum value)	3.40×10^{-8} °C m^{-1} s^{-1}
eff	5.0
h_{max}	22.5 m
γ	5.78×10^{-6} s^{-1}
$\bar{T}_z$ (maximum value)	.036°C m^{-1}

and a linear interpolation of values for intermediate values of x; and also

$$\begin{aligned} M(h') &= h_{\max} && h' > h_{\max} \\ &= -h_{\max} && h' < -h_{\max} \\ &= h' && \text{otherwise.} \end{aligned} \tag{2.4}$$

The parameter η is the SST efficiency of eastern Pacific thermocline displacements while *eff* measures the ratio of the eastern to western Pacific efficiency. The longitudes chosen for defining eastern and western Pacific efficiency regimes are the nearest model grid points to the date line and 140°W. The variation in efficiency is intended to reflect the observed fact that a given upper-level heat anomaly (presumed to be a reasonable proxy for a thermocline perturbation) is associated with much bigger SST anomalies in the east than the west [see, e.g., Inoue et al. (1987)]. A linearization by Hirst (1990) of the ZC model shows this variation is also a feature there with the physical justification being that water at the base of the constant depth mixed layer is less affected by thermocline displacements in the west since the climatological thermocline is deeper. It will also be a feature of any model that assumes a constant entrainment into a mixed layer that shoals from west to east as is observed (see below). In section 5 below, we shall examine the sensitivity of hindcast skill to the efficiency ratio parameter *eff*.

The purpose of (2.4) is to prevent runaway coupled instability and to crudely mimic nonlinear behavior in the system. A nonlinearity very similar to (2.4) was recently used by Münnich et al. (1991) in a study of the effects of nonlinearity on idealized coupled oscillators. A more complicated nonlinearity that essentially has a similar effect in limiting the influence of h' is present in the ZC model and is essential in limiting oscillations to finite amplitude [see Battisti and Hirst (1989) for a good discussion]. The physical justification is that for large enough negative perturbations, the temperature of the subsurface water entrained into the mixed layer becomes equal to the mixed layer temperature and hence no larger negative SST anomalies are possible. Similarly, if the thermocline becomes very deep through a large positive thermocline displacement, entrainment becomes negligible and so no further reduction in entrainment cooling is possible. Clearly, in practice these limits will depend on the mean state of the mixed layer, which varies considerably zonally (see below). We ignore such a complication here and choose a zonally constant $h_{\max}$. Again, however, we test model sensitivity to this parameter.

Turning now to Ekman-induced equatorial upwelling anomalies and their possible influence on SST, we note first the fact that there can be no influence on SST of downwelling and therefore the only influence is a cooling one during upwelling. We write, therefore,

$$EUT(\bar{w}, w') = -[\Delta(\bar{w} + w') - \Delta(\bar{w})]\bar{T}_z$$

$$\bar{T}_z = \frac{(\bar{T} - \bar{T}_b)}{H_m}, \tag{2.5}$$

where Δ is the Heaviside step function and w is the vertical velocity at the base of the mixed layer, which has depth H_m; $\bar{T}_b$ is the climatological value of the subsurface temperature. The above formulation is identical to the one chosen in ZC.

To obtain w we first model the mixed-layer shear flow in an identical manner to ZC, Philips (1987), and Neelin (1991):

$$\gamma u_s - \beta y v_s = \frac{\tau_x}{(\rho_0 H_m)}$$

$$\gamma v_s + \beta y u_s = \frac{\tau_y}{(\rho_0 H_m)}, \tag{2.6}$$

where u_s is the current shear between the mixed layer and the subsurface layer; γ is a strong damping coefficient corresponding to strong vertical mixing. Note that in regions away from the equator for which $f \equiv \beta y \gg \gamma$, the flow is simply the classical Ekman one.

To obtain an expression for w, an expression for the total current in the mixed layer is required. Again we follow ZC and write

$$\underline{u_m} = \underline{u_g} + \frac{H - H_m}{H}\,\underline{u_s}, \tag{2.7}$$

where the subscript g refers to the value derived from the shallow-water equations and H is the depth of the shallow-water layer. Both H and H_m exhibit in reality quite strong zonal variation: the first because of the strong change in stratification from east to west; the second because of a similar zonal trend (see below). Motivated by simplicity, we set the coefficient to a constant value of 2/3, the value used in ZC. The vertical velocity at the base of the mixed layer is then

$$w = H_m \nabla \cdot \underline{u_m} = w_g + \frac{2}{3} w_e, \tag{2.8}$$

where the subscript e refers to the Ekman-induced part of the upwelling. In general, for the parameter choices made in the current model for the shear damping coefficient[1] γ, the second Ekman part of the upwelling is much greater than the first "shallow-water" upwelling. All experiments to be described below were conducted with and without w_g with virtually no change in the results. Therefore, we henceforth ignore w_g.

The evaluation of $\bar{T}_z$ in equation (2.5) is not straightforward. In the ZC model, $H_m = 50$ m and thus

[1] Values required to obtain some measure of agreement with observed and OGCM modeled values of near-surface upwelling velocities.

$\bar{T}_b$ is simply the climatological temperature at 50 m, which can be obtained from data. According to Levitus (1982), however, H_m exhibits reasonably strong zonal variation (being quite shallow in the east). The assumption of constant H_m implies that $\bar{T}_z$ increases markedly from west to east. If on the other hand, we assume that H_m simply corresponds to the depth of near-isothermal surface water, then $\bar{T}_b$ might be assumed to be relatively constant zonally [this is the assumption made by Anderson and McCreary (1985)] and hence $\bar{T}_z$ will depend on the compensating effects of varying H_m and $\bar{T}$. Such an identification of the mixed-layer depth with isothermal depth is probably incorrect in the far western Pacific due to the presence of the so-called "barrier layer," which involves vertical salinity but not temperature fronts (see Lindstrom et al. 1987). It is clear from this discussion that considerable uncertainty attaches to the value for this important parameter. This uncertainty is *crucial* to whether Ekman upwelling has a significant influence on the SST equation or not.

This question has been open since the days of Bjerknes, and according to an excellent recent review by Cane (1992), considerable doubt on the issue still remains. The issue is also an important one in ocean general circulation modeling, as shall be discussed below. In the present context, we adopt the simplest strategy open: we set the value of $\bar{T}_z$ to a constant and then test the sensitivity of our results to justifiable variations in its value (these are discussed below).

It is of some interest to obtain an expression from (2.6) for w_e at the equator:

$$w_e(y=0) = \frac{1}{\rho_0 \gamma}\left(\nabla \cdot \vec{\tau} - \frac{\beta}{\gamma}\tau_x\right). \qquad (2.9)$$

For the observed coherent scales for wind stress, the second term on the right-hand side of (2.7) is generally an order of magnitude larger than the first. This implies that to the extent that the nonlinearity associated with the Heaviside functions in (2.5) can be ignored, that the term EUT is essentially dependent on the local zonal stress anomalies. Manifestations of this term in the SST field may therefore be expected to exhibit a similar locality. We shall return to this point later.

The final parameterization required is zonal advection. This may be written as

$$AT = -\bar{u}_m T'_x - u'_m(\bar{T} + T')_x, \qquad (2.10)$$

where u_m is the equatorial mixed-layer zonal velocity given by (2.7). Unlike the vertical velocity, both the shear and shallow-water zonal horizontal currents are important and we therefore retain both. It is worth pointing out that Philander and Pacanowski (1980) have provided model evidence that nonlinear effects caused by the vertical advection of momentum are probably significant in influencing the above currents. These considerations are beyond the scope of the present publication but nevertheless should be borne in mind when interpreting results. The variables required for evaluating AT are calculated as follows: u_s is calculated using a fixed value for H_m of 50 m, u_g is obtained from the shallow-water equations discussed previously, $\bar{T}$ from the monthly CAC SST climatology, and the current climatology is calculated from a forced model run with climatological winds (see below).

We now discuss observationally plausible values for the crucial model parameters η and $\bar{T}_z$. We first assume a fixed value of 2.72×10^{-7} s^{-1} for ϵ corresponding to a temperature relaxation time scale of around 40 days (see, however, the discussion below). Second, we consider separately the steady-state SST response to a given thermocline displacement (from the term TT) and zonal wind stress change (from the term EUT).

If we assume that the value of $|h'|$ does not exceed $h_{\max}$, then we have in the eastern Pacific:

$$T' = \frac{\eta}{\epsilon} h'. \qquad (2.11)$$

Displacements h' of order 15 m are typical during ENSO extrema when the shallow-water equations are forced with observed wind stress anomalies (see next section), so if a value of 3.40×10^{-8} °C m^{-1} s^{-1} is chosen for η, we should expect a response of about 2°C because the relaxation time scale for the dissipation term is far smaller than the typical length of ENSO events. This response can account for the entire ENSO signal and we will regard it as maximal.

Turning to EUT and assuming that the response region remains one of total upwelling then we have, upon neglecting the first term in (2.7), a steady-state response of

$$T'_s = \frac{K}{\epsilon}\tau'_x$$

with

$$\frac{K}{\epsilon} \equiv \frac{2\beta \bar{T}_z}{3\epsilon\rho_a \gamma^2}. \qquad (2.12)$$

As noted above, γ needs to be set to reproduce observed values of equatorial upwelling. We choose the value of 5.78×10^{-6} s^{-1}. A value for $\bar{T}_z$ of 0.036°C m^{-1} will imply a response of 3°C for a stress anomaly of 0.05 N m^{-2}, which is typical of ENSO extrema. We thus regard this value for $\bar{T}_z$ as the maximal value that can be justified observationally.

Notice that the above considerations are contingent on the value for ϵ. We chose a value that gave a reasonably rapid response time for anomalies compared to the ENSO time scale. In section 5 below we conduct a sensitivity experiment in the pure thermocline case where ϵ is varied but η/ϵ is kept fixed to preserve the steady-state response.

The particular choices decided for model parameters are displayed in Table 1.

Finally we outline the wind forcing and coupling procedure for the model: in order to force the ocean model, the Florida State University (FSU) (Legler and O'Brien 1984; Legler 1987, personal communication) pseudostress product was converted to a stress using $c_D = 1.5 \times 10^{-3}$ and a monthly climatology constructed from the 1972–86 data. Departures from this climatology were calculated and a 1–2–1 filter in time, longitude, and latitude were applied to the result to obtain the product used to force the anomaly ocean model.[2] Where mean quantities were required, they were calculated by forcing the model with total stress for the period 1961–1986 and the appropriate fields were calculated for the same period from which the stress climatology was constructed.

In coupled mode, the SST anomalies [calculated using (2.1) and the fixed meridional structure] were passed to the atmosphere every month where they were superimposed on the monthly CAC SST climatology. The resulting surface wind anomalies were used to construct stress anomalies via the linearized stress law

$$\underline{\tau}' = \rho_a c_D |W| u', \qquad (2.13)$$

with, in general, $|W| = 6.5$ m s^{-1} being the assumed background scalar wind. A linearized rather than fully quadratic stress law was preferred on the grounds of simplicity but also because the model first EOF of zonal wind was judged to show better agreement spatially with the observed first EOF of zonal stress than the corresponding quantity for model stress.

In hindcast experiments, the ocean model was spun up (commencing always in January 1969) to the hindcast date using the stress anomalies described above. Thus, all oceanic variables at the start date for the hindcast are determined by a long history of realistic stress forcing of the ocean model. Following the start date, stress anomalies are provided by the atmospheric model, that is, the model is fully coupled as detailed above. Each hindcast lasts for two years.

3. Upwelling versus thermocline thermodynamics

In this section we vary the SST equation from a regime dominated by Ekman-induced equatorial upwelling to one dominated by thermocline displacements. Zonal advection effects are considered in the next section.

As mentioned in the Introduction, we shall examine the behavior of the ocean model from the viewpoint of forced response, coupled hindcast skill, and also the nature of coupled oscillations.

The precise parametric variations for this section consist of multiplying the maximum observationally justifiable of $\bar{T}_z$ by α and the maximum justifiable value of η by $1 - \alpha$ and varying α from 1 to 0. All other parameters are as displayed in Table 1.

The forced behavior was examined by subjecting equatorial SST anomalies to an EOF analysis. The data consisted of the anomalies from the period 1972–86 produced after forcing the anomaly model from January 1969 to December 1986. The results for the zonal pattern of the first EOFs may be found in Fig. 1a, while the corresponding component time series are in Fig. 1b. The explained variance of the EOF varied smoothly from 60% for $\alpha = 1$ to almost 86% for $\alpha = 0$. The striking feature of the spatial pattern is how the response region changes from the central to eastern Pacific as α decreases. This may be explained as follows: when $\alpha = 1$ the response of the ocean is essentially locally forced by zonal stress anomalies. Above the diagram is a heavy line indicating the longitude of greatest amplitude for the first EOF of observed zonal stress (see Latif et al. 1990). The correspondence between the responses is reasonably close, which supports the above assertion. When $\alpha = 0$ the response is dominated by thermocline displacements, which, as is well known, are phase shifted to the east of their forcing (see, for example, Neelin 1991). The observed (from CAC analysis) first EOF pattern of the 5°N–5°S averaged SST (which explains 69% of the variance) and its component time series can be found in Fig. 1c. For comparison the corresponding quantities for $\alpha = 0$ are also included. It is clear that the spatial pattern shows better qualitative agreement with lower values of α although the pattern extends somewhat farther to the west than in the case $\alpha = 0$. We return to this latter point in the next section when the effects of zonal advection are considered.

The remarkable feature of the component time series is the lack of variation with α. All show reasonable agreement with the observed time series. Evidently, assessing an ocean model from the component time series of its first EOF is not necessarily a very revealing test of performance; the spatial pattern is a better test.

The hindcast skill was assessed next. A sample of 59 two-year hindcasts were obtained with initial conditions every three months commencing January 1972 and ending July 1986. The NINO3 SST index (SST averaged over 5°N–5°S, 150°W–90°W) from the model was compared with the observed values taken from the CAC analysis. Anomaly correlation and rms error skill were computed for the hindcasts and for persistence as follows: Data was stratified with respect to the number of months in the hindcast, that is, one month, two months, etc., following the start date. Thus, 24 samples of 59 NINO3 values were considered. A corresponding set of samples were taken from the observational record and for each of the 24 sample pairs the correlation and rms difference were calculated. In the case of persistence the model samples were replaced

[2] Cardone et al. (1990) have shown that an artificial time trend exists in the FSU data. For the period used here (1972–86) the evidence from an EOF analysis of model SST taken from forced runs (see next section) indicates that this problem is not serious. We thus leave the data untrended.

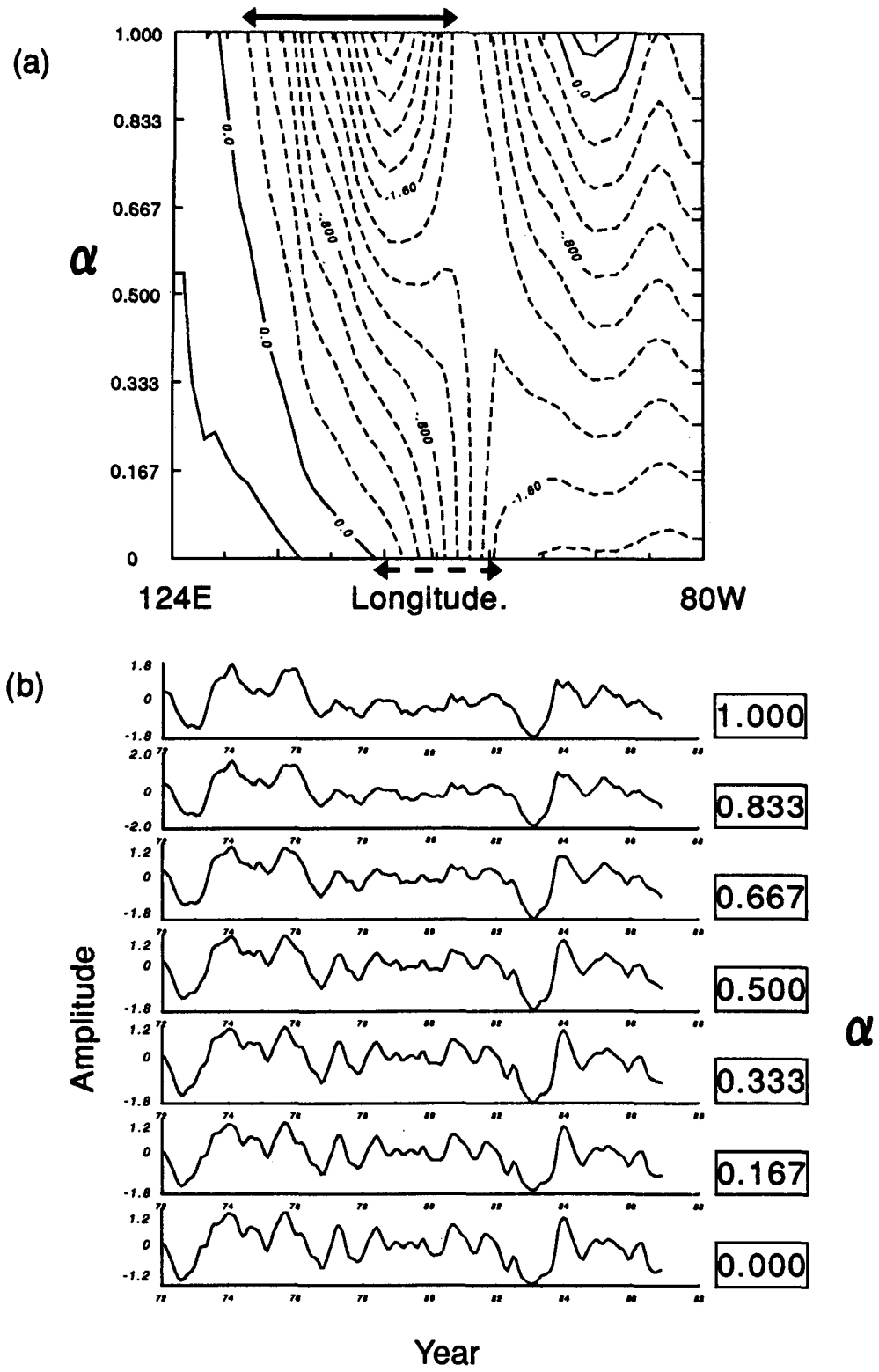

FIG. 1. EOF analysis of upwelling/thermocline experiments. (a) Spatial pattern along the equator for various values of α (see text); contour interval is 0.2. The heavy solid line above the diagram is the region of greatest amplitude of the first EOF of observed wind stress (see text). The heavy dashed line below the diagram corresponds with the transition region for thermocline SST efficiency (see text). (b) The corresponding component time series for the EOFs. (c) The observed first EOF of 5°N–5°S averaged SST together with the corresponding "pure thermocline ($\alpha = 0$)" model equatorial first EOF. The first diagram is the spatial pattern and the second the component time series. The solid lines are the $\alpha = 0$ model.

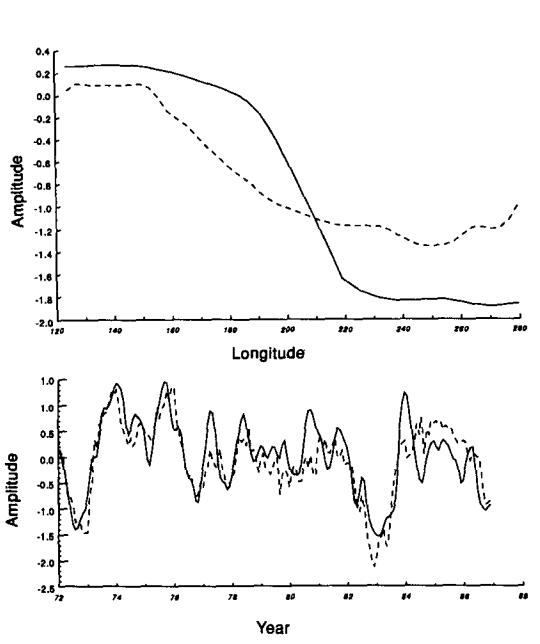

FIG. 1. (*Continued*)

by 24 identical samples with the observational value at the hindcast start date replacing the model value. Persistence hindcasting thus corresponds to always using the observed start date value as a hindcast.

The above test of model performance is stricter than verifying against the *forced* model values. Experience with a range of coupled models has shown that high skill in the second test can often be accompanied by low skill in the more useful first test. This suggests that results from the second test should be treated with caution. Further discussion on the two different tests may be found in Graham et al. (1992).

The anomaly correlation skill curves can be seen in Fig. 2a while the persistence skill is in Fig. 2b with the $\alpha = 0$ skill as reference. A very pronounced pattern is evident with skill increasing unambiguously as α is reduced. For $\alpha = 0$ there are clear indications of skill out to around one year. It is worth noting in this latter case that the correlation at lag 0 is around 0.8, quite a high value, which indicates the forced model is performing well. Persistence is exceeded after around three months which, by definition, must have a correlation of 1.0 at lag 0.

The rms error skill displayed in Fig. 2c (with persistence in 2d) shows a less clear pattern than the anomaly correlation although it is evident for shorter lags that better skill is obtained for values of α less than 0.5. In order to better understand these results and their relation to Fig. 2a, we examine the mathematical relation between rms error E and correlation r (see, e.g., Snedecor and Cochran 1967):

$$E^2 = \sigma_o^2 + \sigma_p^2 + (\mu_o - \mu_p)^2 - 2r\sigma_o\sigma_p, \quad (3.1)$$

where the subscript o denotes an observed value, p refers to the predicted value, σ is the standard deviation, and μ is the mean. Neglecting the third term on the right which is in general small, we note that the rms error depends in a significant way on the variance of the predicted time series. Thus, the explanation for the small variation in E for $0 < \alpha < 0.4$ but large variation in r for the same range is that the variance of the predicted time series declines (quite sharply for small lags) as α increases, and this compensates for the decreasing value of r (which would have increased E if the variance had remained constant). This effect reflects the fact that the coupled behavior becomes more stable as α increases. It is also worth commenting on the rms error at lag 0 which for $\alpha = 0$ looks quite large at 0.72°C. Since $\sigma_p \cong \sigma_o$ at lag 0 we obtain

$$E = (2)^{1/2}\sigma_o(1 - r)^{1/2}. \quad (3.2)$$

It is clear that to halve E would require increasing r from 0.8 to 0.95!

We turn our attention now to the nature of oscillations in the coupled system and how they change as α varies. We confine ourselves to two values for this parameter, namely, 0 and 0.5. This enables some qualitative feel for coupled behavior.

For $\alpha = 0$ the model was allowed to oscillate freely for ten years, commencing July 1982 (the initial conditions were exactly those used for the hindcast commencing on this date), which was the beginning of the large 1982–1983 ENSO. A Hovmöller diagram of model equatorial SST can be found in Fig. 3a. As can be seen, a strong warm event develops and then terminates around a year later to be followed by a moderate cold event. The oscillation induced by the initial conditions decays fairly rapidly after a couple of years showing that the model is basically stable.

A notable feature of the decaying oscillation is its eastward propagation. This is somewhat unrealistic—the observations for 1982–1983 show that a negative anomaly did follow the warm event but was not as active in the central Pacific as the model. In addition, comparison of model predictions for the 1972 and 1987 warm events with observations showed that while the character of the model predictions were much the same as Fig. 3a, the observed anomalies showed virtually no eastward propagation. We shall return to this point when we discuss the effects of zonal advection below.

For the case $\alpha = 0.5$ it was found that the coupled behavior was particularly stable with initial condition anomalies being erased within months. This is consistent with the drop-off in variance with α noted in hindcast experiments above. It was found, however, that as the coupling strength was increased [the parameter $|W|$ in (2.12) was increased] a particular kind of oscillation developed after a few years of coupled integration. The form of this oscillation for $|W| = 9.5$ m s^{-1} can be found in Fig. 3b, which has the same format as 3a. The oscillation shows westward propa-

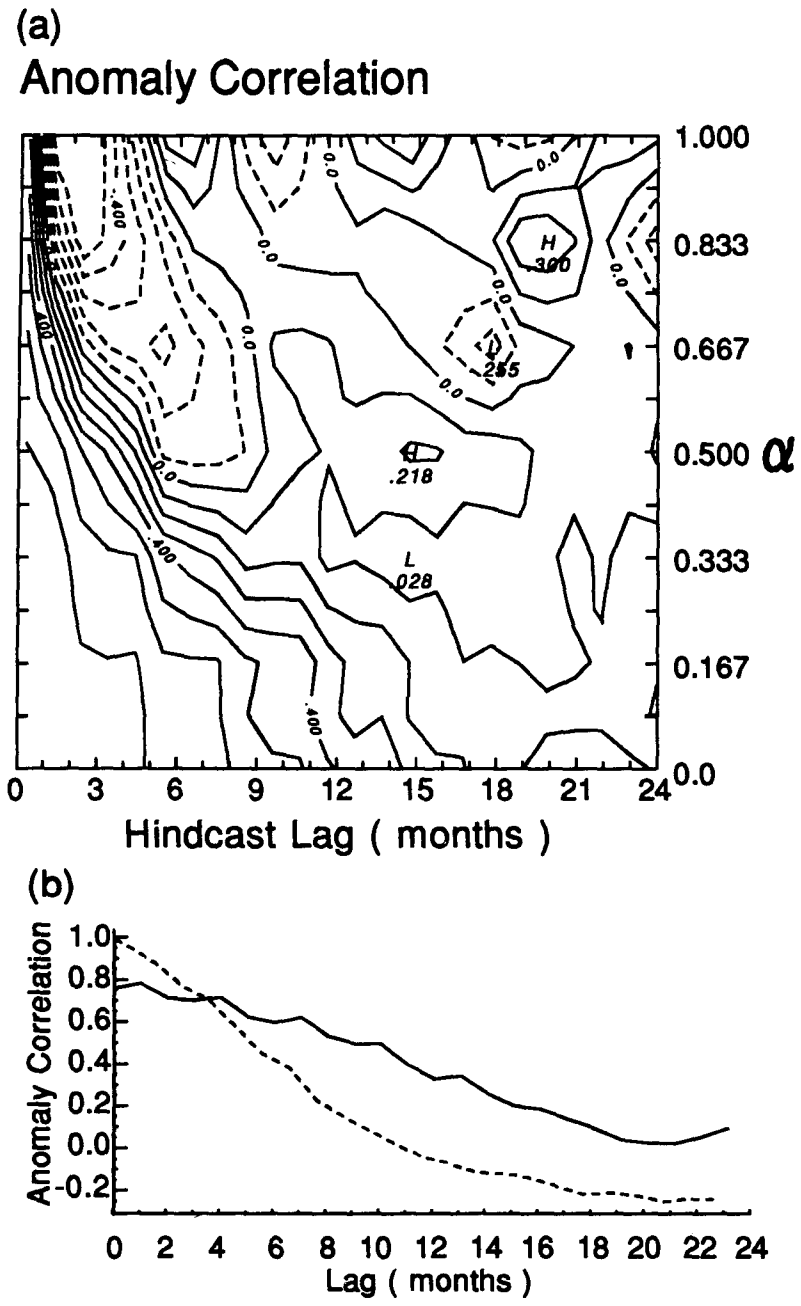

FIG. 2. Hindcast skill at NINO3 for various values of α. (a) The anomaly correlation skill; contour interval is 0.1. (b) The anomaly correlation of the pure thermocline model (solid line) and persistence (dashed line). (c) rms error skill; contour interval is 0.1°C. (d) rms error of the pure thermocline model (solid line) and persistence (dashed line).

gation and has a period of around 18 months. Also notable is the asymmetry between warm and cold phases. The warm events tend to be concentrated in the central/western Pacific while cold events propagate to the western boundary where there is some tendency for them to intensify. In addition, the warm events are around twice the duration of cold events. With respect to the above qualitative features, this oscillation is similar to that previously found both by Kleeman et al. (1992) and Neelin (1991). In both of these latter models, simple atmospheres identical and similar, respectively, to the one used here were coupled to OGCMs. This suggests that both the terms *EUT* and *TT* are important in both of the OGCMs used—a point made by Neelin in the latter publication (and confirmed by the author in the case of the first OGCM). It is also

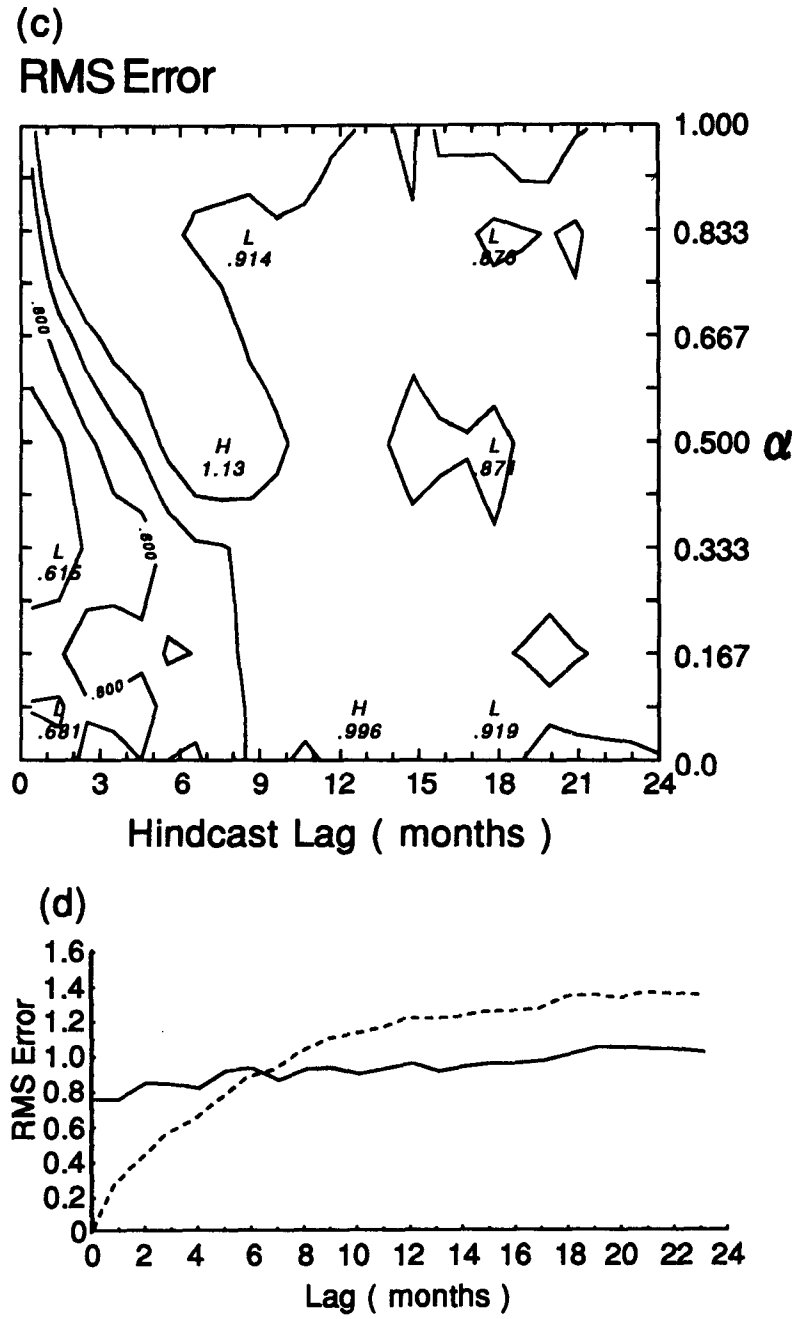

FIG. 2. (*Continued*)

worth noting that the correlation hindcast skill of the first hybrid coupled model above is similar to the skill seen for the case $\alpha \sim 0.5$. The implication of the above for OGCM modeling will be examined in the discussion section below.

4. The effect of zonal advection

The major conclusion of the previous section was that the term TT is primarily responsible for hindcast skill and the term EUT acts to strongly reduce this skill. This implies that a "realistic" value of $\bar{T}_z$ is probably a quite small fraction of the maximal value in Table 1. Because of this conclusion, we ignore the EUT term for the rest of the paper and adopt except where specifically mentioned, the maximal value for η displayed in Table 1. In this section we examine the influence on coupled behavior of including the term AT with TT.

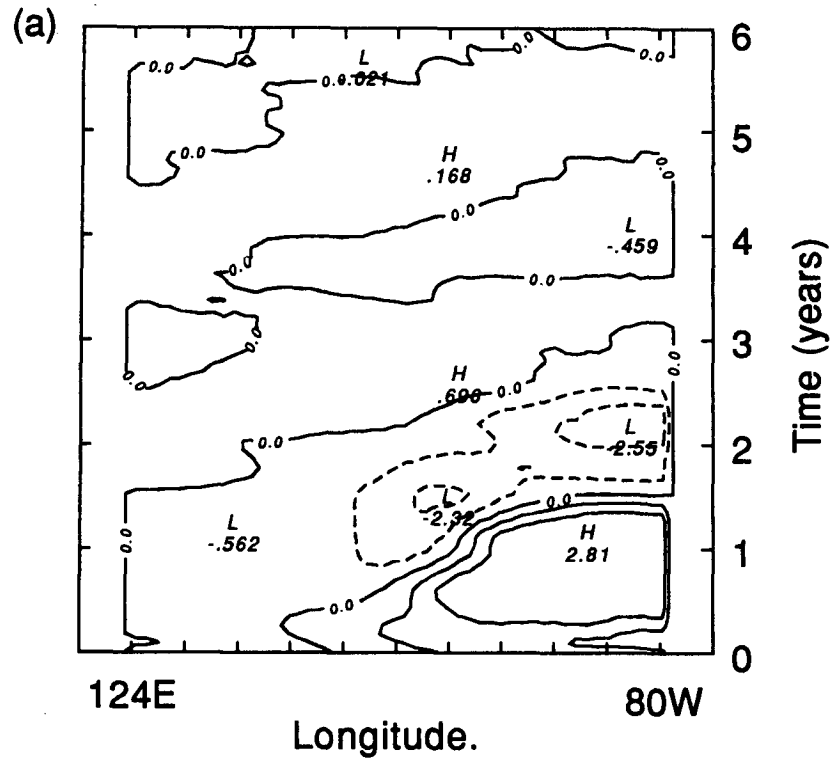

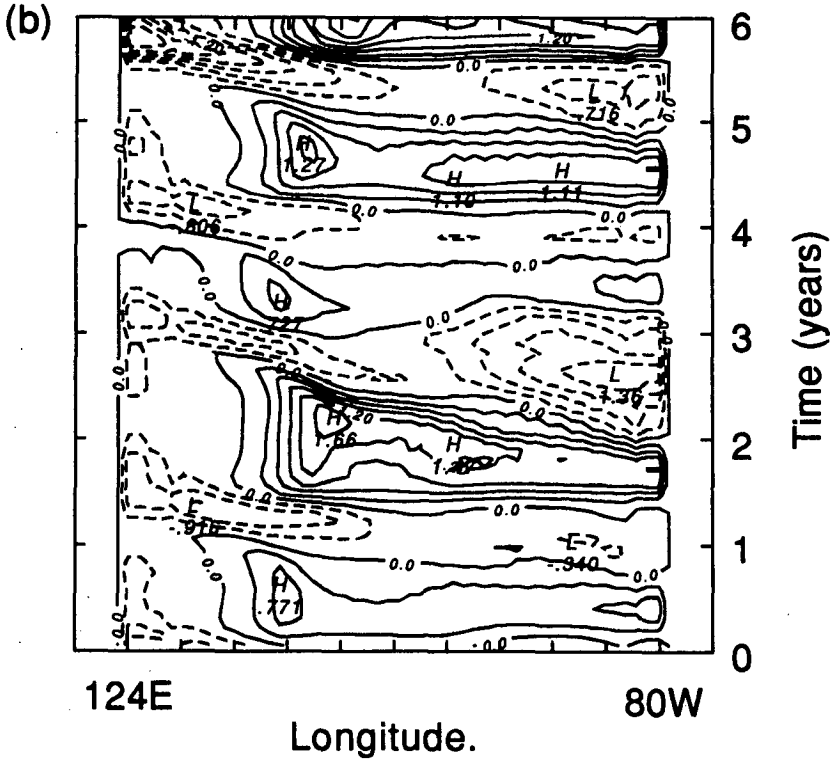

FIG. 3. Hovmöller diagrams of model SST for six-year periods (see text). (a) Pure thermocline model; contour interval 1.0°C. (b) The case $\alpha = 0.5$; contour interval 0.3°C.

Specifically the maximal value of η was multiplied by the eight factors (1., 1., 1., 1., 0.75, 0.5, 0.25, 0.), while the AT term was multiplied by (0., 0.33, 0.67, 1., 1., 1., 1., 1.). This method represents a gradual ramping in of zonal advection followed by a removal of the influence of thermocline displacements.

As in the previous section, the forced behavior was first examined. The first EOF of SST was calculated and accounted for a declining percentage of the variance as zonal advection became more important. Nevertheless, in all cases, more than 50% of the variance was explained. The spatial patterns can be found in Fig. 4a, where three features stand out: first, as the zonal advection becomes more important, the western edge of the pattern shifts to the west (and hence initially agrees better with the observations); second the magnitude of the response diminishes sharply after η is reduced from its maximal value; finally, the strongest response remains in the east for all but the last two settings where it shifts to the center of the basin.

The component time series displayed in Fig. 4b show little variation except for the last two settings where there is a sharp degradation in agreement with the observations.

Turning now to the anomaly correlation hindcast skill located in Fig. 5a, we note that for the first four settings there is a mild decline in skill at short time lags with a given correlation level occurring around two months earlier for the fourth as opposed to the first setting. For longer lags there is some hint of increased skill up to the third setting.

The rms error (Fig. 5b) shows a large increase for the first four settings and then a sharp decline subsequently. This can be primarily understood through equation (3.1) and the standard deviation pattern (Fig. 5c). This latter quantity shows a large increase as zonal advection is ramped in and a strong decline as η declines. The explanation is that the coupled model becomes more unstable with the zonal advection term added but less stable as TT, the major contributing term (see the forced response above) to SST, is reduced. Possible explanations for the increased instability when zonal advection is increased include the increased zonal extent of the SST anomaly [lower zonal wavenumbers tend to be more unstable for thermocline thermodynamics: see Hirst (1986)] and the possibility of larger SST anomalies through the new term (anomalies due to TT are restricted by the nonlinearity).

We consider finally the oscillatory behavior. Illustrated in Fig. 6a is a six-year run of the fourth setting initialized at July 1982. As can be seen, relative to the first setting there is somewhat less evidence of eastward propagation and also evidence of slightly greater zonal extent. The agreement with observations of the 1982–83 event is better as a result. Other events (for example, 1987 and 1972) show the same structure in the model but a less propagating pattern in the observations. The above effects can be more clearly seen by increasing somewhat the coupling strength parameter $|W|$ in (2.12) to 8.5 m s^{-1}. In both the pure thermodynamics case (Fig. 6c) and the fourth setting (Fig. 6b) self-sustaining oscillations develop. The final six years of runs commencing at July 1982 are displayed. As is evident from a comparison with Figs. 3a and 6a, the nature (aside from growth/decay) of the oscillations are little changed by increasing the coupling strength. The reduced eastward propagation and greater zonal extent in the zonal advection case is now evident. In these respects the addition of zonal advection has increased the realism of the oscillation.

5. Dependence of skill on the thermocline parameterization

Given that hindcast skill seems to derive primarily from the SST effects of thermocline perturbations, it is of interest then to see how sensitive this skill is to the details of the parameterization of TT. We consider here five different tests of this sensitivity:

(a) zonal variation in the "efficiency" of thermocline perturbations in causing SST anomalies,
(b) western boundary reflections,
(c) nonlinearity,
(d) the response time of SST to a given thermocline perturbation,
(e) the shallow-water speed.

a. Zonal asymmetry

We vary the value of $1/eff$ in (2.3) from a value of 1 to 0. This corresponds to a variation from zonally uniform thermocline efficiency to a situation where western Pacific SST is insensitive to thermocline perturbations.

As in the previous section we begin by considering the forced behavior of the model. The first EOF of model SST was calculated and the spatial pattern is shown in Fig. 7. The explained variance of this EOF is again always high and varies monotonically from 88% for $1/eff = 0.$ to 72% for $1/eff = 1.0$. The spatial pattern shows that as the thermocline efficiency becomes more zonally uniform, western Pacific SST anomalies of the opposite sign to the eastern Pacific anomalies become evident. When the efficiency is uniform this response is about the same magnitude as the eastern Pacific response, which is not in agreement with observations (see section 3). This confirms the usefulness of the Λ factor used in (2.1) in giving a better SST response. The component time series (not shown) show virtually no sensitivity to eff.

Looking now at the correlation hindcast skill variation (Fig. 8a), we observe that there is not a large dependence of skill on eff. For lags of nine months or less, it is evident that larger values of eff are in general better to the extent that a given correlation level occurs

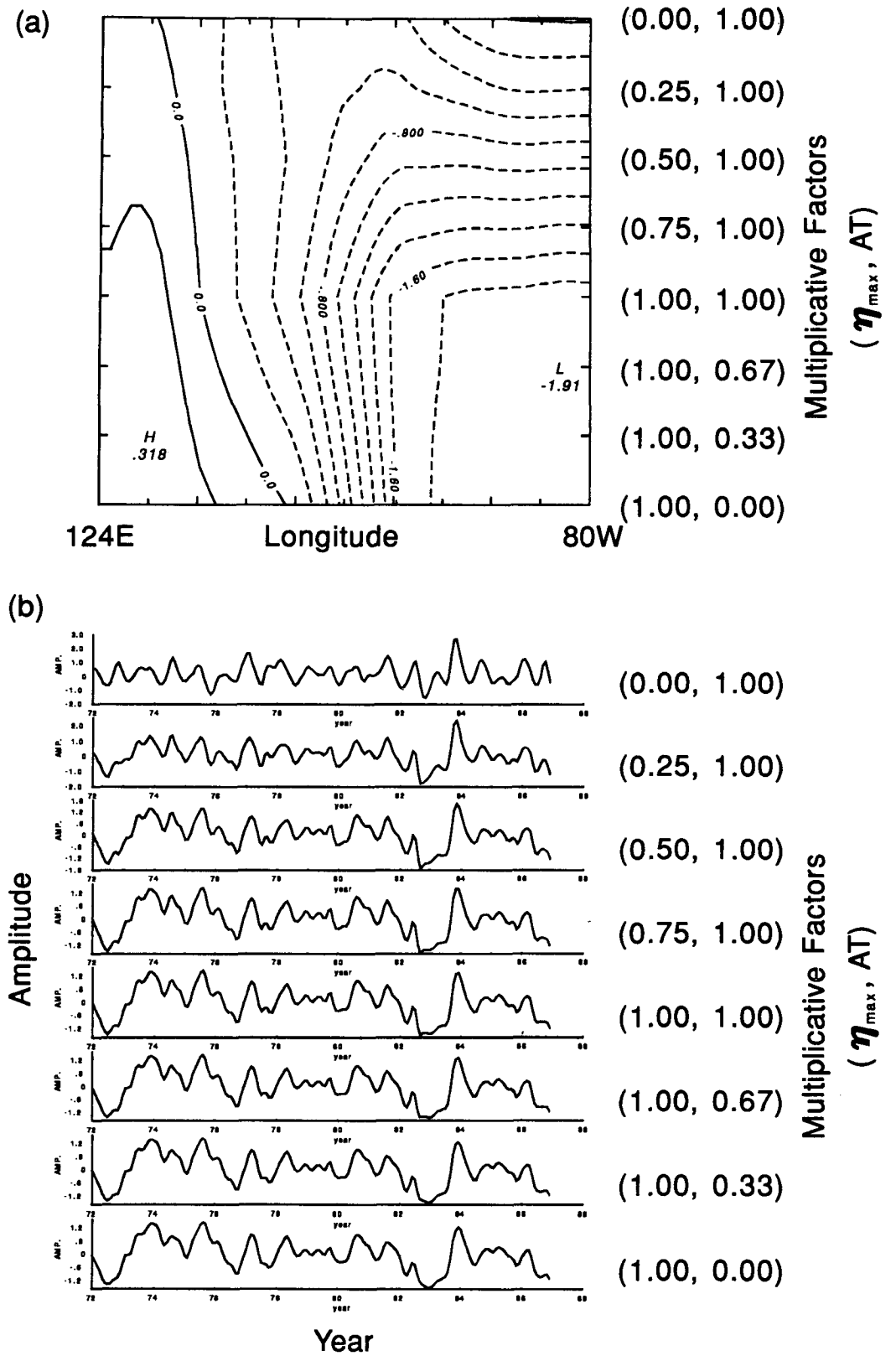

FIG. 4. EOF analysis for the thermocline/zonal advection experiments (refer to text).
(a) Spatial pattern of first EOF; contour interval 0.2. (b) Component time series corresponding to (a).

around two months later than in the zonally uniform case.

The pattern of rms error (Fig. 8b), as in previous experiments, shows a different picture with a general increase in error as *eff* is reduced. This tendency is particularly pronounced at longer lags where the error essentially doubles between *eff* = 3 and *eff* = 2. Examination of the variance of hindcasts (not shown) shows that for longer lags (>1 year) there is also a dramatic increase (from 0.2 to >2.0) over this parameter range and this serves to explain the increase in error (see previous section). The explanation for this behavior, as in the previous section, is that the coupled model becomes more unstable over the above parameter range with the nonlinear parameterization (2.4) preventing runaway and restricting the oscillation to finite amplitude. To confirm the above analysis, a run with *eff* = 2.0 was carried out with $|W|$ reduced from 6.5 m s^{-1} to 4.5 m s^{-1}. The anomaly correlation was not affected to any significant degree but there was a large decrease in rms error, particularly for longer lags.

Turning to oscillatory behavior, we examine a six-year run with *eff* = 2.0 to illustrate the typical behavior at low values of *eff*. This can be seen in Fig. 9 where a pronounced pattern is evident: a finite-amplitude oscillation propagating eastward with a period of just over three years. The oscillation is very regular and is most intense in the eastern half of the basin, presumably because *eff* > 1. There also seems to be some evidence of asymmetry between warm and cold phases, which increases to the west.

b. *Western boundary reflections*

This sensitivity experiment allows Rossby waves to radiate away from the Pacific basin. The first EOF pattern and component time series were computed as before but did not show a sensitivity to the western boundary (not shown).

The only differences of note from the standard model are a somewhat greater amplitude of the eastern basin response relative to the western one and the fact that the 1973 and 1975 cold events are not as well separated without the boundary.

In contrast to the above weak sensitivity in the forced case, the coupled behavior as manifested by hindcast skill and the long-term coupled oscillatory behavior response show a dramatic change. Figure 10 shows the anomaly correlation and rms error. We note in the first case a large decline in skill after around two months. It is fascinating, however, to notice the closeness of the skill to the standard model for these first two months. It is worth observing that this time scale is approximately that for the gravest mode Rossby wave to propagate from the central Pacific to the western boundary and return as a Kelvin wave. The rms error shows a strong growth after a month or so and saturates after 10 months at a quite high level. The explanation for this behavior can be found in the long-term oscillatory behavior displayed in Fig. 11, which was initialized at the beginning of the 1982–1983 warm event (July 1982): the model initially grows in a very similar manner to the standard model but then locks in a permanent warm event. The lack of oscillatory behavior caused by the absence of a time-delayed negative feedback from the western boundary seems to be responsible for the decline in skill and also the greater instability (which causes large rms errors). It is worth noting that when this sensitivity experiment was performed on a model with no zonal contrast in thermocline thermodynamical efficiency (i.e., with *eff* = 1.), a regular eastward-propagating oscillation of period 3–4 years was altered to a permanent warm event. This strongly suggests that zonal asymmetry in ocean thermodynamics (at least with respect to thermocline changes) is not the reason for the appearance of the western boundary sensitive mode here as has been suggested by Hirst (1990). This point is examined further in the discussion section below.

c. *Nonlinearity*

Nonlinearity was examined by altering h_{max} from 22.5 m (which induces a steady-state SST anomaly of around three degrees) to 15 and 30 m. Larger values of h_{max} than this latter value are not acceptable in the current model because SST anomalies could occur in the coupled model that the atmospheric model cannot treat correctly [total temperature cannot approach 32°C—see Kleeman (1991)].

In summary, the impact of these changes was essentially restricted to altering the amplitude: in the forced case the amplitude of the first EOF was greater for larger values of h_{max}. The correspondence of the normalized component time series was almost exact except at the peak of the 1982–1983 warm event where the larger value of h_{max} gave a larger event (relative to the 1972 event).

The model hindcast skill (see Fig. 12) shows little sensitivity in the anomaly correlation but larger rms errors for larger values of h_{max}, which again is what one would expect from larger-amplitude coupled behavior.

Confirming this point, the coupled oscillations (commencing at July 1982) conformed to this pattern with little change in the character of the oscillation as h_{max} changes but the amplitude varying essentially linearly with h_{max}.

d. *SST response time*

In this sensitivity experiment, the response time of SST anomalies to thermocline perturbations was varied by changing ϵ but also adjusting η so that their ratio remained constant. This ensured that the response magnitude remained approximately constant [see Eq.

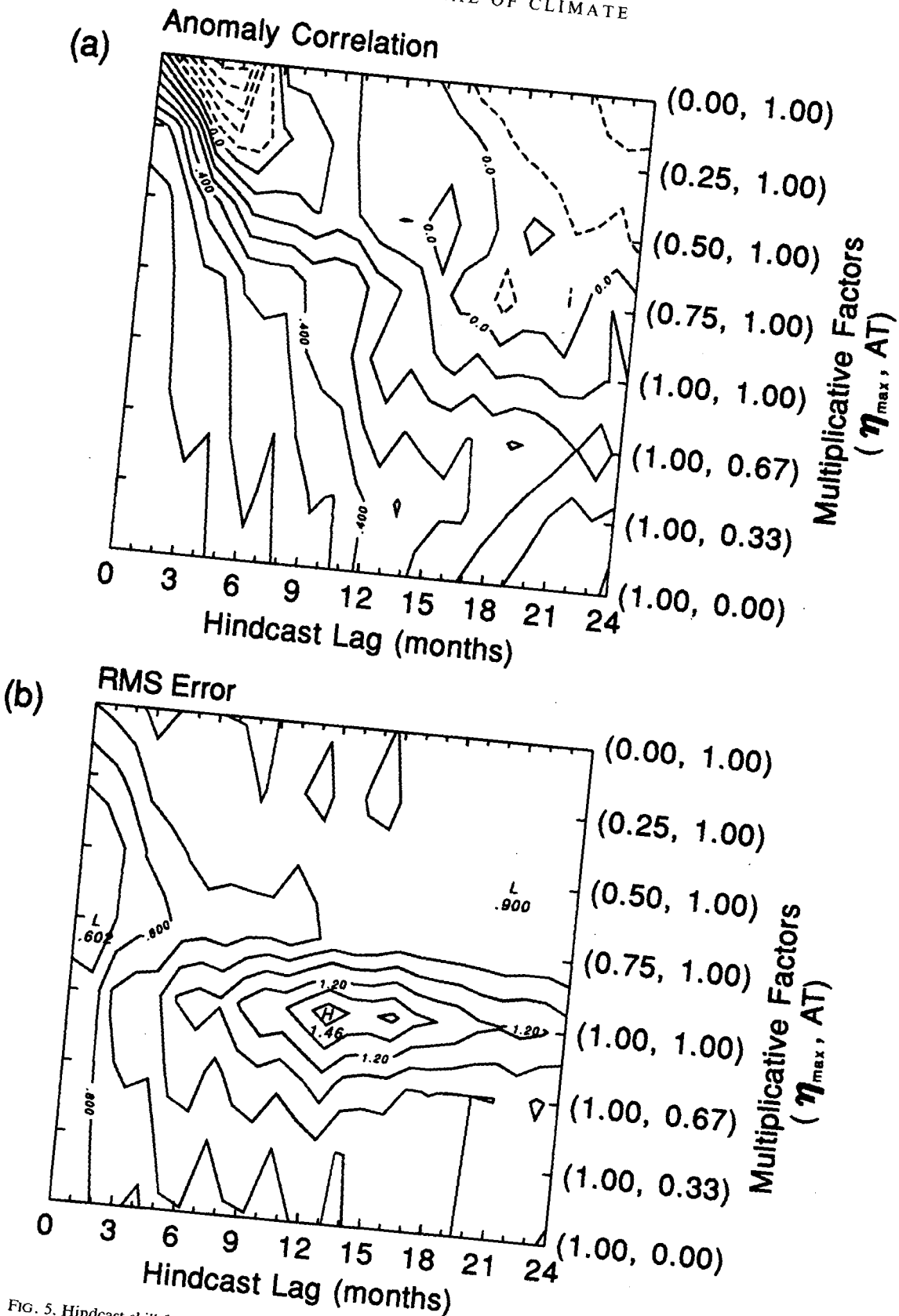

FIG. 5. Hindcast skill for the thermocline/zonal advection experiments. (a) Anomaly correlation skill; contour interval 0.1. (b) rms error; contour interval 0.1°C. (c) Standard deviation of hindcasts; contour interval 0.1°C.

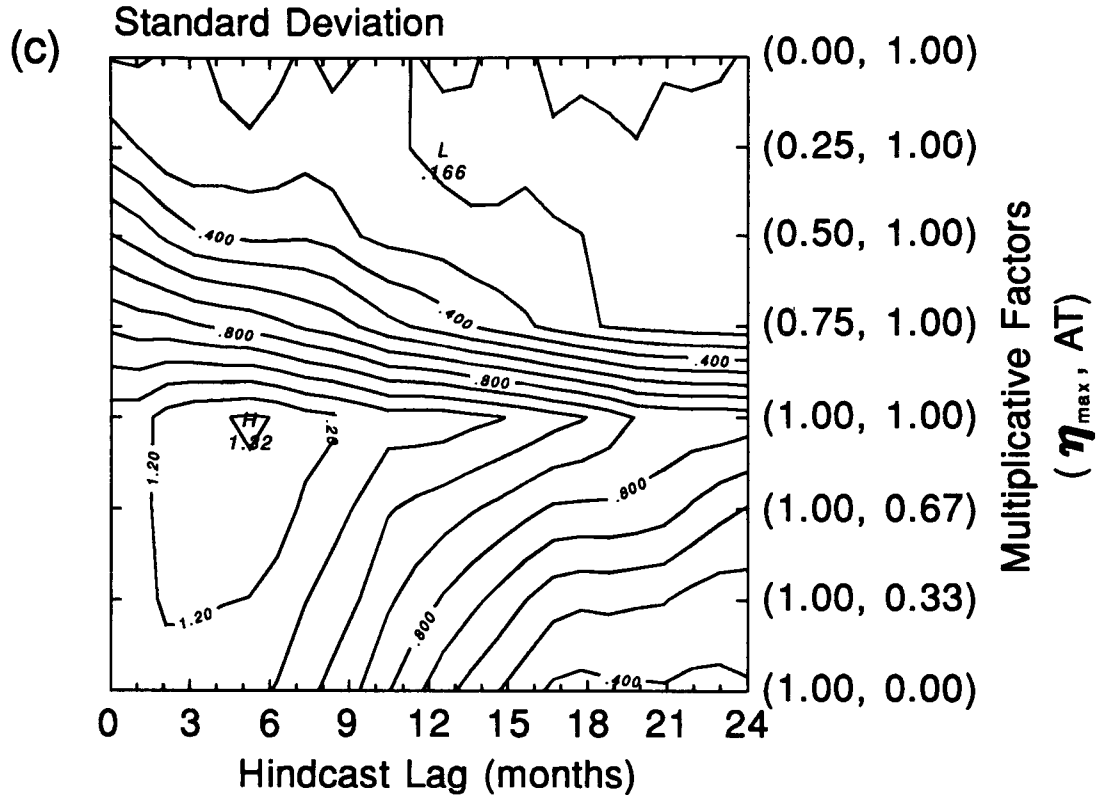

FIG. 5. (*Continued*)

(2.10)]. Denoting by ϵ_s the value of ϵ in the standard model, the following parameter settings were chosen: $\epsilon = (3.0, 2.0, 1.67, 1.0, .83, .67, .47, .33)\epsilon_s$. This corresponds to varying ϵ^{-1} from ~2 weeks to ~4 months.

The first EOF was calculated for the forced case and accounted for greater than 80% of the variance for all the settings. The spatial pattern of the EOFs (not shown) shows virtually no sensitivity to the parametric variation. On the other hand, the component time series shows some variation. As the response time becomes longer, the time series becomes smoother and also the phase shifts forward in time by a few months.

With respect to anomaly correlation hindcast skill (Fig. 13a) there is a small amount of sensitivity evident with best performance, at lags of 4–12 months, being for response times of 1–2 months. At longer lags there is a hint that longer response times are better. The rms error (Fig. 13b) shows an unambiguous decline as response time increases. As before, examination of the variance shows that this is the primary cause, again apparently because the model is more unstable for shorter response times.

The oscillatory behavior of the models was examined by taking a six-year period initialized at July 1982. Two parameter settings were examined corresponding to long and short response times ($\epsilon = 2\epsilon_s$ and $.47\epsilon_s$) with the results displayed in Figs. 14a and 14b. As can be seen, the decaying oscillations evident in both runs have different periods with the longer period corresponding to the longer response time. The qualitative character of the oscillations remains unaffected.

e. Shallow-water speed

The sensitivity of behavior to the value chosen for a shallow-water speed was seen as a worthy area of study because Cane (1984) has demonstrated that in order to account for the observed ENSO sea level anomalies with a linear model, the first two vertical modes are required. In his model these had shallow-water speeds of 2.91 m s^{-1} and 1.78 m s^{-1} so one might expect a single-mode model with an intermediate value to perform better. Of course a better test of this issue would be to successively include the higher vertical modes in the model. We defer such a study to a future publication and simply vary the shallow-water speed from $c = 3.3$ m s^{-1} to 1.5 m s^{-1}.

As previously, the forced model first EOF was calculated and accounted for greater than 80% of the variance in all cases. There was no sensitivity of the spatial pattern to c. On the other hand there was some sensitivity in the component time series. In general, the smaller the value of c the smoother the series; in ad-

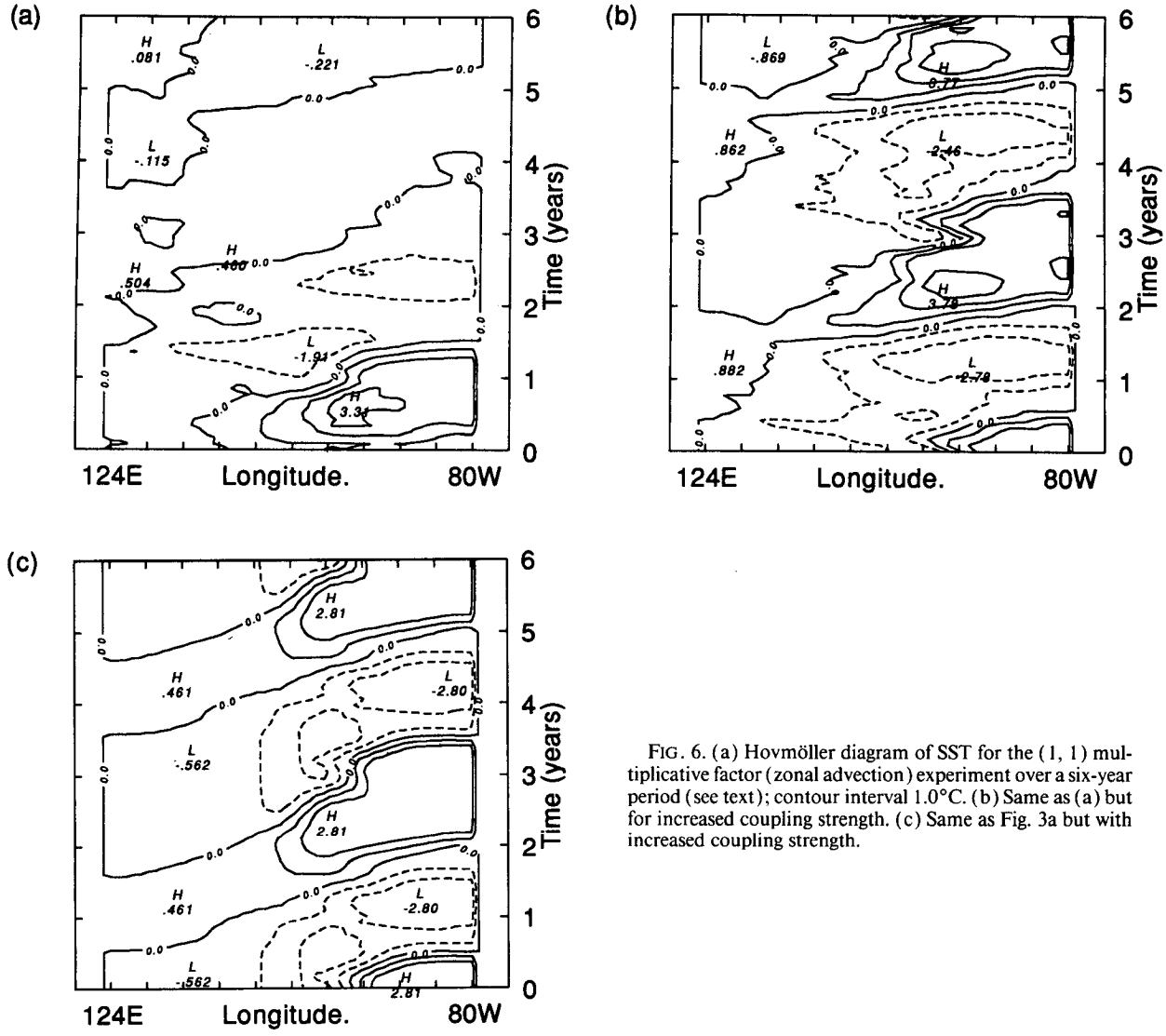

FIG. 6. (a) Hovmöller diagram of SST for the (1, 1) multiplicative factor (zonal advection) experiment over a six-year period (see text); contour interval 1.0°C. (b) Same as (a) but for increased coupling strength. (c) Same as Fig. 3a but with increased coupling strength.

dition, a phase shift amounting to a few months occurs between the highest and lowest speeds with features occurring later in the latter case.

Examining anomaly correlation skill (Fig. 15a) we see that our perhaps naive expectation above has been met. The optimal setting appears to be around 2.2 to 2.4 m s^{-1} with the increase in skill being more apparent at longer lags where there is a hint of skill in the second year of the hindcasts. The falloff in skill about this setting for lags less than a year is more pronounced for smaller values of c.

The rms error (Fig. 15b) shows little variation above 1.7 m s^{-1} but below this value there is a sharp increase, particularly at intermediate lags. Examination of the variance (not shown) shows a gradual increase to larger values ($\sim$1.) for smaller values of c. This suggests that the model is more unstable for lower values of c.

The oscillatory behavior was examined for c = 3.3 m s^{-1} and 1.5 m s^{-1} with the observation that, relative to the standard model case, the period of the damped oscillation increased as the shallow-water speed decreased. The general form of the behavior was, however, unaltered.

In most respects there was a symmetry between this sensitivity experiment and the last with decreasing response time giving a similar sensitivity to increasing shallow-water speed.

6. Summary and discussion

A "family" of simple coupled models of the tropical Pacific has been constructed with a fixed atmosphere (which shows good agreement with observations) and a series of ocean models whose thermodynamics vary.

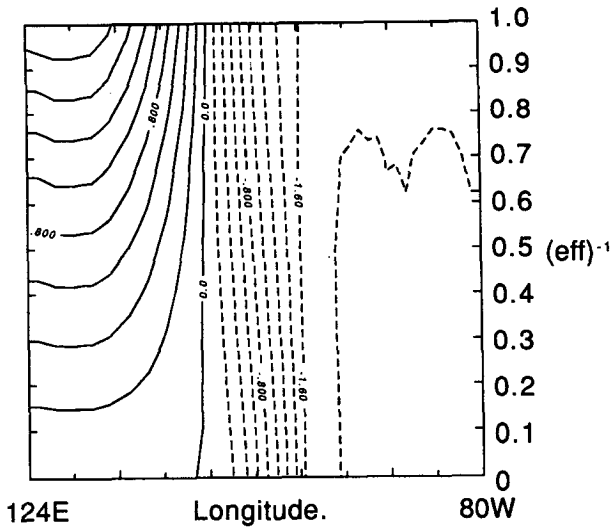

FIG. 7. Same as Fig. 4a but for the zonal asymmetry experiments.

This has been done to isolate the essential features required in an ocean model for a coupled model to exhibit realism. Realism has been assessed here mainly by examining hindcast skill, but also by looking at forced ocean and long-term oscillatory coupled behavior.

The principal result is that high hindcast skill is dependent on the SST equation being dominated by the influence of thermocline perturbations that are in general a remote response to wind forcing. Additionally it has been found that western boundary reflections are critical to hindcast skill in the range of 2 to 12 months. Such a result strongly suggests that negative feedbacks generated by the western boundary are essential to realistic coupled behavior and thus lends support to the mechanism lying behind the "delayed action oscillator" ENSO paradigm as proposed by Suarez and Schopf (1988) and refined by Cane et al. (1990) and Schopf and Suarez (1990).

An important negative result obtained is that the realism of the coupled model declines sharply as Ekman-induced upwelling (which is, to a good approximation, a local response to wind forcing) effects begin to significantly influence the SST equation. Since this term has been identified by Neelin (1991) and Philander et al. (1992) (see also Kleeman et al. 1992) as an important one in some ocean general circulation models, further investigation of this effect would seem warranted. The present coupled model, with approximately equal contributions to the SST equation from the upwelling and thermocline terms, shows qualitative similarity in its coupled and hindcast skill behavior to a "hybrid" coupled model described in Kleeman et al. (1992). This latter coupled model involves the atmosphere used here together with the Max-Planck-Institut für Meteorologie tropical Pacific general circulation model as described in Latif and Villwock (1990).

This coupled oscillation is also quite similar to that reported by Neelin (1990) except that the period is around 1.5 years here against 3 years in the Neelin hybrid coupled model. It would seem therefore that overexcitation of this coupled mode, which is of quite different character than the "delayed action oscillator" coupled mode seen in the ZC model, can seriously compromise realism. It is tempting therefore to speculate that such a mode is not an important part of the current observed coupled system.

A somewhat similar sensitivity of coupled behavior to ocean thermodynamics has also been found in coupled general circulation models. When the same AGCM was coupled to a coarse global and fine-resolution tropical Pacific OGCM (Lau et al. 1992; Philander et al. 1992, respectively) ENSO oscillations of

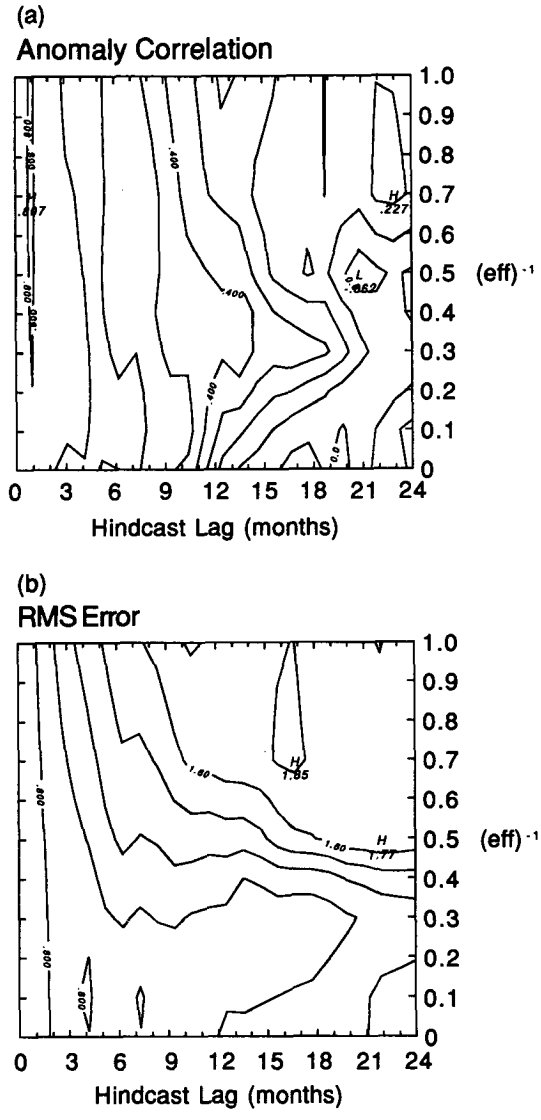

FIG. 8. Same as Fig. 5 but for the zonal asymmetry case.

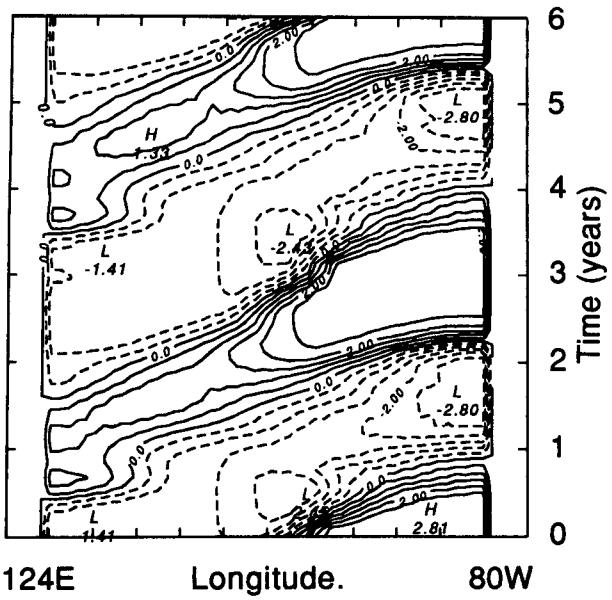

FIG. 9. Hovmöller diagram of SST for the case *eff* = 2 (see text); contour interval 0.5°C.

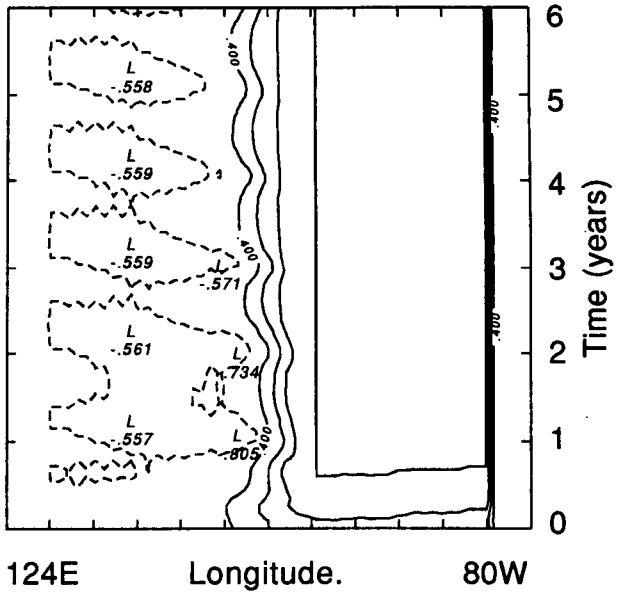

FIG. 11. As in Fig. 3a but for the standard model with western boundary removed; contour interval 0.8°C.

quite different characteristics were seen. According to Philander et al. the reason for the difference in behavior is the prominence of the term wT'_z in the temperature equation of the upper layers of the fine-resolution model and its virtual absence in the coarse case. The interpretation given to this term is the influence of thermocline perturbations on SST (this follows because such perturbations are manifest in the OGCM as subsurface temperature anomalies and are "brought to the surface" essentially by the model upwelling). In the coarse-resolution model Lau et al. demonstrate that

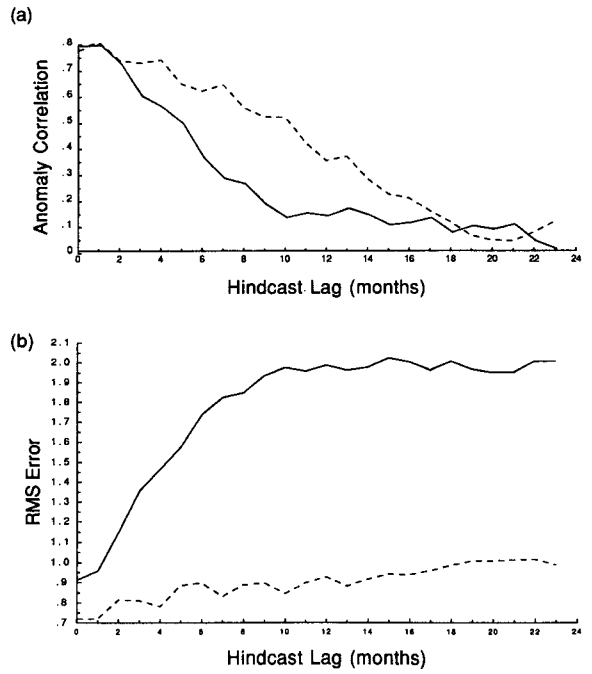

FIG. 10. Hindcast skill in the case of western boundary removal; solid line is the no-western boundary case while the dashed line is the standard model. (a) Anomaly correlation; (b) rms error.

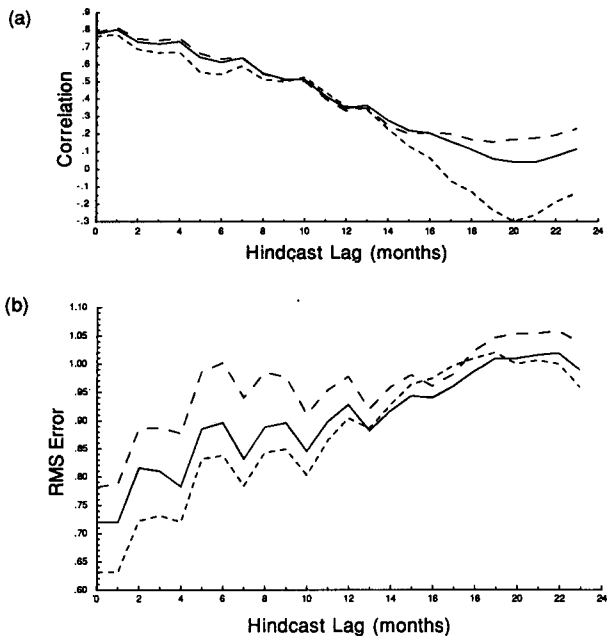

FIG. 12. As in Fig. 10 but for nonlinearity. Solid line is the standard model, short dash is the reduced h_{max} case, while long dash is the increased case (see text).

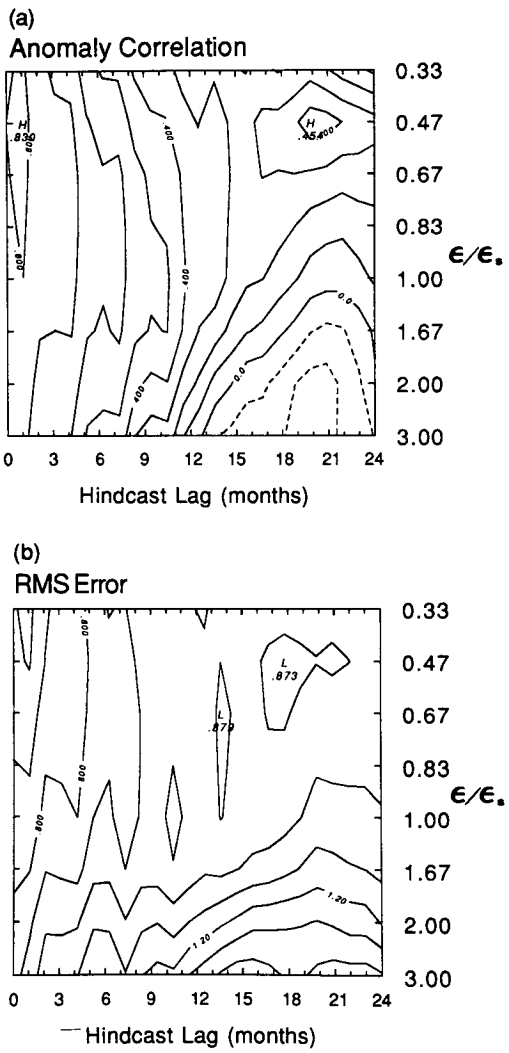

FIG. 13. Same as Fig. 5 but for the varying thermal response time experiments.

the terms that are essentially *locally* driven by winds ($u'\bar{T}_z$ and $w'\bar{T}_z$) are particularly important, and this helps to explain the westward-propagating character of the oscillations.

The current results provide strong evidence that dominance of thermocline perturbations in the SST equation (which is a remote response to wind forcing) is required for realistic coupled behavior. Hindcast skill is a particularly stringent and objective means of assessing realism. The idea of thermocline perturbation dominance has been raised repeatedly in the literature [see, e.g., Seager 1989; Münich et al. 1991; and ZC]. The evidence provided here is particularly strong because of the fact that a coupled model containing only this effect and in a particularly simple form survives a very rigorous test of its realism.

With regard to other sensitivities, it was found that the forced *and* oscillatory behavior is somewhat improved by the inclusion of zonal advection. Surprisingly perhaps, there was however a mild decline in anomaly correlation hindcast skill. Given the crudeness of the zonal current formulation [the results of McCreary (1981) and Philander (1980) strongly suggest that more complicated models are required] such a paradoxical result is perhaps to be expected. Minor deficiencies in the atmospheric model such as the overstrong far eastern Pacific winds may also be responsible.

The small sensitivity of anomaly correlation hindcast skill to zonal asymmetry in the SST "efficiency" of thermocline perturbations was rather interesting and suggests that such asymmetries are *not* fundamental to coupled behavior of the current model. As the results of the previous section show, the zonally symmetric model shows a very strong sensitivity to western

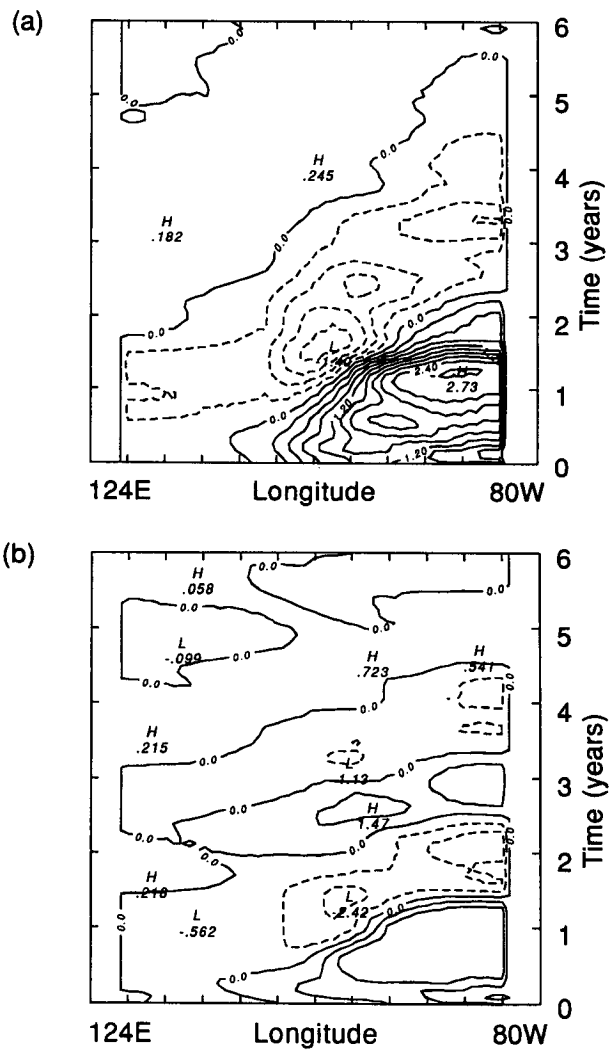

FIG. 14. As in Fig. 3a but for the standard model with increased and reduced thermal response times (see text). (a) Increased response time; contour interval 0.3°C. (b) decreased response time; contour interval 1.0°C.

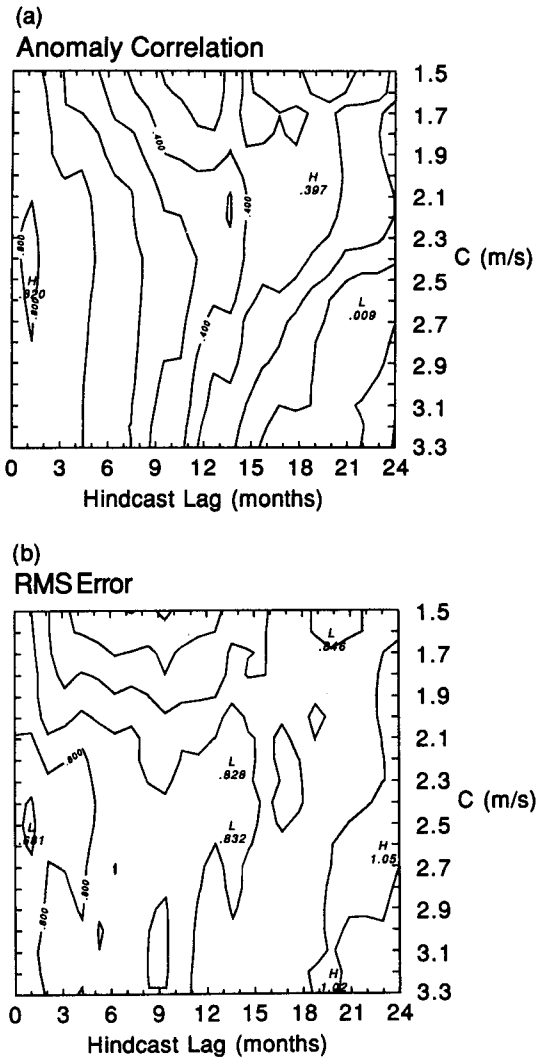

FIG. 15. Same as Figs. 5a and 5b but for the varying shallow-water speed experiment.

boundary reflections suggesting that it is a "propagating delayed action oscillator" and not a so-called SST mode discussed by Neelin (1991).[3] This result seems to be at variance with the results of Hirst (1988), who has shown that the most unstable mode in a finite basin has a similar structure to that observed here but is not sensitive to western boundary reflections (A. Hirst 1992, personal communication). The temperature equation used by Hirst differs in two respects from the one deployed here in that the parameters η and ϵ have different values (η is an order of magnitude larger here) and the present equation contains a nonlinearity. These, together with the nonlinear atmosphere used here [Hirst used a linear Gill (1980) model with heating proportional to SST anomaly], seem to be the only possibilities for this fundamental difference in behavior.[4] The fact that the oscillation seen here has regions of peak SST with $|h| \geqslant h_{\max}$ suggests that thermocline nonlinearity is likely to be important. If $h_{\max}$ is varied as in the previous section a similar behavior to the one reported there occurs in the zonally symmetric oscillation. The amplitude responds proportionately but the period and character remains unaltered. Such behavior has been reported previously by Battisti and Hirst (1989) in their nonlinear delayed-action oscillator analog of the ZC model.

The mild sensitivity of hindcast skill to the relaxation time of SST to thermocline anomalies seems to be connected with the variation in the period of the coupled modes produced. A realistic period of 3–4 years seems to give the best skill, as intuition would suggest.

Finally, the sensitivity of particularly the long lag hindcast skill to variations in the shallow-water speed was suggestive. As Cane (1984) has pointed out, the first two vertical modes with shallow-water speeds of 2.91 m s^{-1} and 1.78 m s^{-1} are required on both theoretical and observational grounds to adequately model ENSO sea level anomalies and hence probably thermocline perturbations. This conclusion seems to be indicated for coupled models also since an intermediate shallow-water speed compared to the values mentioned above performed best.

A number of conclusions and avenues of further investigation flow naturally from the above results. First, since thermocline perturbations are at the heart of realistic coupled behavior it would seem that a good depiction of OGCM upper-level equatorial thermal structure should be an important consideration for modelers. This conclusion has been drawn previously for other reasons by modelers [see, e.g., Smith (1991) on the relevance of these considerations to data assimilation into OGCMs]. The fact that the mean thermal structure in the regions of Ekman upwelling determines the strength of the EUT term [see (2.5)] through its determination of $\bar{T}_z$ also emphasizes the above point.

With regard to the hindcast skill seen here it is very reassuring for future efforts to forecast ENSO that, apart from Ekman upwelling, there was remarkably little sensitivity (using NINO3 anomaly correlation as a yardstick) to the details of the parameterizations deployed here. Compared to the ZC model (B. N. Goswami 1992, personal communication) the optimal model seen here (standard model with a reduced shallow-water speed) showed greater anomaly correlation skill for the first seven months; equal skill in the range of 7 to 12 months; and greater skill beyond this.

[3] Such a mode arises solely from the SST equation and is not dependent on wave effects.

[4] I am indebted to Tony Hirst for a discussion on this point and also to comments by an anonymous reviewer.

One obvious avenue for model improvement involves the introduction of more vertical modes. Not only will an "intermediate" value of the shallow-water speed be produced naturally, but as McCreary (1981) has shown, a better zonal current model will also result.

Acknowledgments. The author wishes to thank Mojib Latif of MPI for initiating an interest in the nature of hindcast skill in coupled models. Useful discussions with Neville Smith and Scott Power of BMRC and Tony Hirst of CSIRO have also contributed.

REFERENCES

Anderson, D. L. T., and J. P. McCreary, 1985: Slowly propagating disturbances in a coupled ocean–atmosphere model, *J. Atmos. Sci.*, **42,** 615–629.

Battisti, D. S., 1988: The dynamics and thermodynamics of a warm event in a coupled atmosphere/ocean model. *J. Atmos. Sci.*, **45,** 2889–2919.

——, and Hirst, A. C., 1989: Interannual variability in a tropical atmosphere–ocean model: Influence of the basic state, ocean geometry and nonlinearity. *J. Atmos. Sci.*, **46,** 1687–1712.

Cane, M. A., 1984: Modelling Sea Level During El Nino. *J. Phys. Oceanogr.*, **14,** 1864–1874.

——, 1991: Forecasting El Niño with a geophysical model. *Teleconnections Linking Worldwide Climate Anomalies,* M. H. Glantz, R. W. Katz and N. Nicholls, Ed., Cambridge University Press, 345–369.

——, 1992: Tropical Pacific ENSO models: ENSO as a mode of the coupled system. *Climate System Modelling,* K. E. Trenberth, Ed., Cambridge University Press, 583–614.

——, M. Münnich, and S. E. Zebiak, 1990: A study of self-excited oscillations of the tropical ocean atmosphere system. *J. Atmos. Sci.*, **47,** 1562–1577.

Cardone, V. J., J. G. Greenwood, and M. A. Cane, 1990: On trends in historical marine wind data. *J. Climate,* **3,** 113–127.

Chao, Y., and S. G. H. Philander, 1991: On the Structure of the Southern Oscillation and evaluation of coupled ocean-atmosphere model. *TOGA Notes,* April, 1–8.

Gill, A. E., 1980: Some simple solutions for heat induced tropical circulation. *Quart. J. Roy. Meteor. Soc.*, **106,** 447–462.

Goswami, B. N., and J. Shukla, 1991: Predictability of a coupled ocean-atmosphere model. *J. Climate,* **4,** 3–22.

Graham, N. E., T. P. Barnett, and M. Latif, 1992: Considerations of the predictability of ENSO with a low-order coupled model. *TOGA Notes;* April, 11–15.

Harrison, D. E., W. S. Kessler, and B. S. Giese, 1989: Ocean circulation model hindcasts of the 1982–83 El Niño: Thermal variability along ship of opportunity tracks. *J. Phys. Oceanogr.*, **19,** 397–418.

Hirst, A. C., 1986: Unstable and damped equatorial modes in simple coupled ocean–atmosphere models. *J. Atmos. Sci.*, **43,** 606–630.

——, 1988: Slow instabilities in tropical ocean basin–global atmosphere models. *J. Atmos. Sci.*, **45,** 830–852.

——, 1990: On simple coupled ocean–atmosphere models, equatorial instabilities, and ENSO. *Proc. International TOGA Scientific Conference,* Honolulu, WCRP-43; 103–110.

Inoue, M., W. B. White, and S. E. Pazan, 1987: Interannual variability in the tropical Pacific prior to the onset of the 1982–83 El Niño. *J. Geophys. Res.*, **92,** 11 671–11 679.

Kleeman, R., 1991: A simple model of the atmospheric response to ENSO SST anomalies. *J. Atmos. Sci.*, **48,** 3–18.

——, M. Latif, and M. Flügel, 1992: A hybrid coupled tropical atmosphere ocean model: sensitivities and hindcast skill. Max Planck Institut für Meteorologie Report No. 76, 37 pp. [Available from Bundesstraße 55, 2000 Hamburg 13, Germany.]

Kraus, E. B., Ed., 1977: *Modelling and Prediction of the Upper Layers of the Ocean.* Pergamon Press, 325 pp.

Latif, M., and Villwock, A., 1990: Interannual variability in the tropical Pacific as simulated in coupled ocean-atmosphere models. *J. Mar. Syst.*, **1,** 51–60.

——, and M. Flügel, 1991: An investigation of short range climate predictability in the tropical pacific. *J. Geophys. Res.*, **96,** C2, 2661–2673.

——, J. Biercamp, H. von Storch, M. J. McPhadden, and E. Kirk, 1990: Simulation of surface wind anomalies with an AGCM forced by observed SST. *J. Climate,* **5,** 509–521.

Lau, N. C., S. G. H. Philander, and M. J. Nath, 1992: Simulation of ENSO-like phenomena with a low-resolution coupled GCM of the global ocean and atmosphere. *J. Climate,* **5,** 284–307.

Legler, D. M., and J. J. O'Brien, 1984: *The Atlas of Tropical Pacific Wind Stress Climatology 1971–1980.* Florida State University.

Levitus, S., 1982: Climatological Atlas of the World Ocean. NOAA Prof. Pap. No. 13; U.S. Govt. Printing Office, 173 pp.

Lindstrom, E., R. Lukas, R. Fine, E. Firing, S. Godfrey, G. Meyers, and M. Tsuchiya, 1987: The Western Equatorial Pacific Ocean Circulation Study. *Nature,* **330,** 533–537.

McCreary, J., 1981: "A linear stratified ocean model of the equatorial undercurrent." *Philos. Trans. Roy. Soc. London,* **298,** 603–635.

Meehl, G. A., 1990: Seasonal cycle forcing of El Niño–Southern Oscillation in a global, coupled ocean-atmosphere GCM. *J. Climate,* **3,** 72–98.

Münnich, M., M. A. Cane, and S. E. Zebiak, 1991: A study of self-excited oscillations of the tropical ocean–atmosphere system. Part II: Nonlinear cases. *J. Atmos. Sci.*, **48,** 1238–1248.

Neelin, J. D., 1990: A hybrid coupled general circulation model for El Niño studies. *J. Atmos. Sci.*, **47,** 674–693.

——, 1991: The slow sea surface temperature mode and the fast wave limit: Analytical theory for tropical interannual oscillations and experiments in a hybrid coupled model. *J. Atmos. Sci.*, **48,** 584–606.

——, M. Latif, M. A. F. Allart, M. A. Cane, U. Cubasch, W. L. Gates, P. R. Gent, M. Ghil, C. Gordon, N. C. Lau, G. A. Meehl, C. R. Mechoso, J. M. Oberhuber, S. G. H. Philander, P. S. Schopf, K. R. Sperber, A. Sterl, T. Tokioka, J. Tribbia, and M. A. Zebiak, 1992: Tropical air–sea interactions in general circulation models. *Climate Dyn.*, **7,** 73–104.

Oberhuber, J. M., 1993: Simulation of the Atlantic Circulation with a Coupled Sea Ice-Mixed Layer-Isopycnal General Circulation Model. Part I. Model description. *J. Phys. Oceanogr.*, **23,** 808–829.

Pacanowski, R. C., and S. G. H. Philander, 1981: Parameterization of vertical mixing in numerical models of tropical oceans. *J. Phys. Oceanogr.*, **11,** 1443–1451.

Philander, S. G. H., and R. C. Pacanowski, 1980: The generation of equatorial currents. *J. Geophys. Res.*, **85,** 1123–1136.

——, T. Yamagata, and R. C. Pacanowski, 1984: Unstable air–sea interactions in the tropics. *J. Atmos. Sci.*, **41,** 604–613.

——, R. C. Pacanowski, N. C. Lau, and M. J. Nath, 1992: Simulation of ENSO with a global atmospheric GCM coupled to a high-resolution, tropical pacific ocean GCM. *J. Climate,* **5,** 308–329.

Philips, P. J., 1987: A simple model of the wind-driven tropical ocean. *J. Phys. Oceanogr.*, **17,** 2003–2015.

Seager, R., 1989: Modeling tropical Pacific sea surface temperature: 1970–87. *J. Phys. Oceanogr.*, **19,** 419–434.

Snedecor, G. W., and W. G. Cochran, 1967: *Statistical Methods.* The Iowa State University Press, 593 pp.

Schopf, P. S., and M. A. Cane, 1982: On equatorial dynamics, mixed layer physics and sea surface temperature. *J. Phys. Oceanogr.*, **13,** 917–934.

——, and M. J. Suarez, 1990: Ocean wave dynamics and the time scale of ENSO. *J. Phys. Oceanogr.*, **20,** 629–645.

Smith, N. R., 1991: Assimilation experiments using a Pacific Ocean general circulation model. BMRC Research Report No. 27, 174–184. [Available from GPO Box 1289K, Melbourne 3001, Australia.]

Suarez, M. J., and P. S. Schopf, 1988: A delayed action oscillator for ENSO. *J. Atmos. Sci.*, **45,** 3283–3287.

Zebiak, S. E., 1990: Intermediate models of ENSO. *Proc. Int. TOGA Scientific Conference* WCRP-43, 95–101.

——, and M. A. Cane, 1987: A model El Niño Southern Oscillation. *Mon. Wea. Rev.*, **115,** 2262–2278.